

# Chapter 2

## Vacuum Technology

**Abstract** A majority of micro or nano fabrication processes are conducted under partial vacuum conditions, i.e., at pressures orders of magnitude below ambient atmospheric pressure. This is done, among other, to avoid a contamination of films during their deposition. Since the pressure in the vacuum chamber during a pump-down passes through up to 13 orders of magnitude, it is not surprising that rather different gas flow conditions have to be mastered. A look at gas properties and gas flow basics provides an essential understanding for these conditions. A vacuum system reaching ultrahigh vacuum consists of a combination of at least two pumps, a roughing pump working in the viscous flow regime and a high-vacuum pump working down to the molecular flow regime. Typically, roughing pumps are displacement pumps, while high-vacuum pumps are either kinetic transfer pumps or entrapment pumps. General vacuum issues covered are the vacuum seal, vacuum measurement and analysis, as well as desorption and leaks. A discussion of vacuum pump applications concludes this chapter.

### 2.1 Introduction into Vacuum Technology

#### *2.1.1 Importance of Vacuum Technology for Processing and Characterization*

A majority of processes for fabricating microelectromechanical systems (MEMS) and nanoelectromechanical systems (NEMS) are conducted under partial vacuum conditions, i.e., at pressures orders of magnitude below ambient atmospheric pressure. There are two key reasons for this necessity. The first one is to provide the atoms with a free path in a line-of-sight process, in which they are traveling directly from a source to a substrate to be coated or etched. During the travel, the atoms are subject to collisions with gas molecules present in the process chamber. If the number of collisions with these gas molecules is too large, the atoms lose a substantial amount of their energy. They then either would barely reach the target, with

**Table 2.1** Vacuum phases

Degree of vacuum	Pressure range	
	[Pa]	[Torr]
Rough	$10^5 > p > 10^2$	$750 > p > 7.5 \times 10^{-1}$
Fine	$10^2 > p > 10^{-1}$	$7.5 \times 10^{-1} > p > 7.5 \times 10^{-4}$
High	$10^{-1} > p > 10^{-5}$	$7.5 \times 10^{-4} > p > 7.5 \times 10^{-8}$
Ultrahigh	$10^{-5} < p$	$7.5 \times 10^{-8} < p$

Source O’Hanlon [1], Umrath [2], Ohring [13]

no energy left for traveling to an appropriate position in a crystal structure (in case of a deposition process) or would be incapable of causing a sufficient momentum transfer at the bombarded surface (in case of a physical etching process), respectively. The second reason is minimizing the impingement of air or other gas molecules at the target surface, causing contamination [1].

What, strictly speaking, is vacuum? It is a space completely free of matter. Such a condition neither exists naturally on earth (and not even in outer space), nor is it achievable by technical means. Absolute vacuum does not exist. This was postulated even in the middle ages when it was stated that nature abhors vacuum (Latin: horror vacui). Therefore, an atmosphere with a pressure below ambient strictly speaking is a “partial vacuum”, although we may simply call it “vacuum”. To allow a classification of the subatomic pressure areas, partial vacuum ranges were defined. Table 2.1 provides a common breakdown of the vacuum regime [2]. It should be mentioned that, depending on the source, the names of vacuum regimes and boundaries between them occasionally vary.

Vacuum technology has a multitude of applications. Figure 2.1 presents examples and their pressure ranges, varying from analysis applications to space simulation [2]. Figure 2.2 illustrates the space simulation lab of the Karlsruhe Institute of Technology (KIT) in Eggenstein-Leopoldshafen, Germany, where atmospheric conditions are simulated under various pressure conditions.

### 2.1.2 Historical Overview

One of the first scientists engaged in vacuum was Evangelista Torricelli (1608–1647) [3, 4]. In 1641, he was hired to assist the aging Galileo Galilei (1564–1642) shortly before Galilei died [5]. He investigated as of why suction pumps are not able to raise the water more than 10 m. He concluded that the water in a tube was pushed up by the ambient pressure of the atmosphere and not sucked by vacuum. He continued this work after Galilei had passed away and conducted an experiment. By using mercury, which is 13.5 times denser than water, he reasoned the atmospheric pressure should only be able to push up the mercury 1/13.5 times or about 750 mm. To verify this assumption, he completely filled a glass tube which was closed at the bottom with mercury and covered the top with a plug. Then he

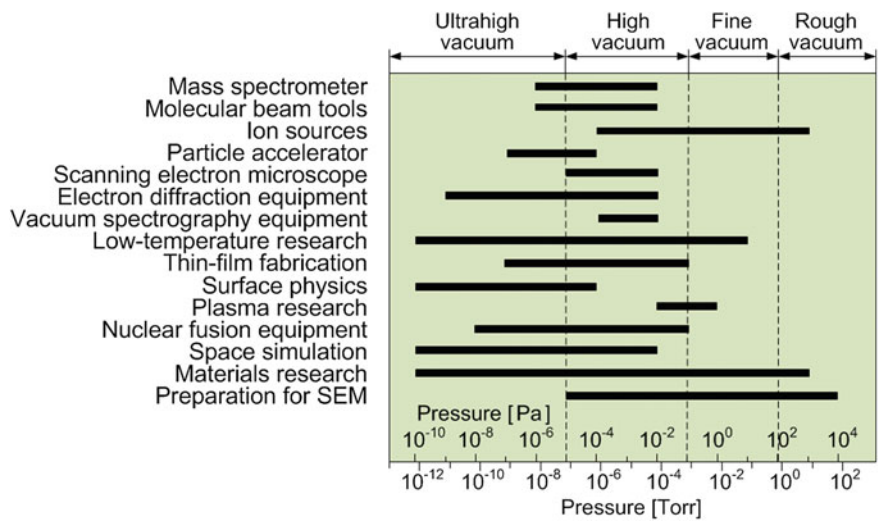
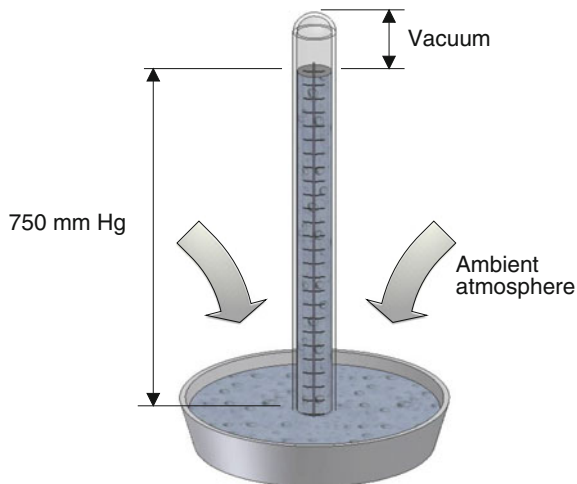


Fig. 2.1 Industrial vacuum usage (adapted from Umrath [2])



Fig. 2.2 Karlsruhe Institute of Technology's AIDA (Aerosol Interaction and Dynamics in the Atmosphere) facility. Pressure range:  $10^2$ – $10^5$  Pa

**Fig. 2.3** Evangelista Torricelli's experiment



placed the tube upside down in a bowl of mercury and removed the plug. Mercury poured out of the tube and a mercury column of approx. 750 mm remained in the tube (Fig. 2.3). The top of the tube was free of mercury—the first creation of a vacuum. In creating this experiment, Torricelli invented the mercury barometer.

Around 1650 Otto von Guericke (1602–1686), burgomaster of Magdeburg, Germany, invented the vacuum pump [6, 7]. He used it to demonstrate the effect of atmospheric pressure. At the Reichstag in Regensburg in 1654, he showed that two hemispheres with a diameter of  $\frac{3}{4}$  Magdeburg cubit (500 mm), with the space between them evacuated, could not be pulled apart by two teams of eight horses each (Fig. 2.4) [8].<sup>1</sup>

Modern high-vacuum technology is considered to start in 1905 with the German physicist Wolfgang Gaede (1878–1945) and his invention of the rotating vacuum pump [9]. He needed vacuum to conduct research on the Volta effect (i.e., the contact potential of a metal. The contact potential is the potential an electron has to overcome when performing a transition from vacuum to the surface of a metal, a phenomenon that would be hard to observe at ambient pressure conditions [10]). A cooperation with E. Leybold's Nachfolger in Cologne, Germany, (and predecessor of Oerlikon Leybold Vacuum) resulted in a commercialization of Gaede's invention between 1906 and 1908 [11]. The cooperation was very beneficial for both sides, in particular since Gaede systematically conducted research regarding alternate vacuum pump principles, thereby inventing the molecular pump in 1912, the diffusion pump in 1915, and 1935 to utilize gas ballast on rotary vane pumps, which allows to pump gases containing a substantial amount of condensed vapor [2].

<sup>1</sup> The originals of both pump and hemispheres are preserved at the Deutsches Museum in Munich, Germany.

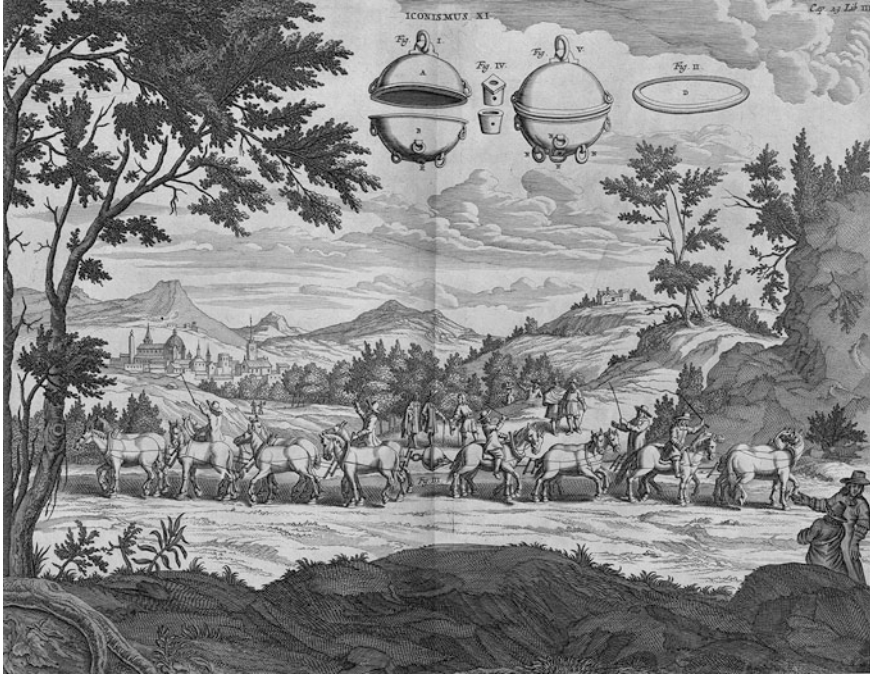


Fig. 2.4 Otto von Guericke's experiment (Sketch by Gaspar Schott [8])

### 2.1.3 Vacuum Technology Basics

#### 2.1.3.1 Ideal Gas Law

For gases at not too high pressures and temperatures, there are rather simple relationships between their physical units [12, 13]. The Anglo-Irish philosopher and writer Robert Boyle (1627–1691) [14] and the French physicist Edme Mariotte (1620–1684) [15] postulated that for a given temperature, the volume of a gas varies inversely with its pressure or, formulated differently, the product of volume and pressure is proportional to the mass  $m$  and a function of the (absolute) temperature  $T$ :

$$pV = f(T) \quad (2.1)$$

The French chemist and physicist Joseph-Louis Gay-Lussac (1778–1859) discovered in 1802 that for a constant pressure  $p$ , the volume  $V$  is a function of temperature  $T$  [16]. This also means that the quotient of  $p$  and  $T$  is constant:

$$\frac{p}{T} = C \quad (2.2)$$

Equations (2.1) and (2.2) may be combined and extended to

$$pV = mR_{\text{spec}}T, \quad (2.3)$$

which represents the equation of state for ideal gases, also named ideal gas law.  $p$  [N/m<sup>2</sup> = Pa] is the pressure,  $V$  [m<sup>3</sup>] the volume,  $m$  [kg] the mass,  $R_{\text{spec}}$  [J/kg·K] the specific gas constant (which is a function of the gas species), and  $T$  [K] the absolute temperature.

Particularly valuable is the ideal gas equation in its molar form. To get to it, we are multiplying a species' specific gas constant with the species' molecular mass  $M$ :

$$R_{\text{spec}}M = R \quad (2.4)$$

While  $R_{\text{spec}}$  is a function of the gas species,  $R$  is not; it is the universal gas constant with the value

$$R = 8.3144621 \text{ [J/mol·K] or [kJ/kmol·K]}. \quad (2.5)$$

Combining Eqs. (2.3) and (2.4) results in the molar form of the ideal gas equation

$$pV = \frac{m}{M}RT = \nu RT. \quad (2.6)$$

The ratio  $m/M$  describes the number of moles  $\nu$  present in volume  $V$ .

### 2.1.3.2 Avogadro's Number and Boltzmann's Constant

According to the hypothesis of the Italian mathematical physicist Amadeo Avogadro, conte di Quaregna e Cerreto (1776–1856), same volumes of ideal gases at equal state of  $p$  and  $T$  contain the same numbers of molecules [13, 17]. Vice versa, for ideal gases a certain quantity of substance (containing a certain number of molecules) has an equal volume.

Avogadro's number (or constant)  $N_A$  describes how many molecules a mol of gas consists of. It equals the number of atoms contained in 12 g of a pure C<sup>12</sup> nuclide and is a subject of substantial international research for constant refinement. According to the Encyclopædia Britannica, Avogadro's number is [18]

$$N_A = 6.02214129 \times 10^{23} \text{ mol}^{-1} \quad (2.7)$$

or

$$N_A = 6.02214129 \times 10^{26} \text{ kmol}^{-1}. \quad (2.7a)$$

The quotient of  $N_A$  and  $R$  is Boltzmann's constant  $k_B$ , named after the Austrian physicist Ludwig Eduard Boltzmann (1844–1906) [1, 19]:

$$k_B = \frac{R}{N_A} \quad (2.8)$$

$$k_B = 1.3804 \times 10^{-23} \text{ J/K} \quad (2.8a)$$

### 2.1.3.3 Particle Density

The particle density  $n$  [ $\text{m}^{-3}$ ] represents the number of atoms or molecules present within a given volume  $V$  [ $\text{m}^3$ ], divided by the volume size [13]. According to the kinetic gas theory (see below),  $n$  is a function of the pressure  $p$  [Pa], Boltzmann's constant  $k$  [J/K], and the thermodynamic temperature  $T$  [K]. For ideal gases, the relationship is as follows:

$$n = \frac{p}{k_B \cdot T} = \frac{\rho}{m_T} \quad (2.9)$$

Equally,  $n$  is a function of the density  $\rho$  [ $\text{kg/m}^3$ ] and a gas molecule's mass  $m_T$  [kg].

### 2.1.3.4 Pressure (Definition)

To conclude the vacuum technology basics, let us have a closer look at the pressure  $p$ . It is defined as the force  $F$  [N] per unit area  $A$  [ $\text{m}^2$ ] [1]. The pressure  $p$  is a scalar (and therefore the force  $F$  always attacks at a right angle) given by

$$p = \frac{F}{A}. \quad (2.10)$$

The SI unit (International System of units) for pressure is  $\text{N/m}^2$ , which is called Pascal (Pa). A unit still in use although obsolete is [13]

$$1 \text{ Torr (mmHg – mm of mercury)} = 133.3224 \text{ Pa}. \quad (2.11)$$

It dates back to Torricelli's experiments and honors him by naming a unit for pressure after him. The total pressure  $p_t$  comprises the sum of all partial pressures  $p_i$ . The partial pressure of a gas or vapor equals the pressure that a gas or vapor would exhibit if it were the sole constituent inside the container.

## 2.2 Gas Properties

### 2.2.1 Kinetic Gas Behavior

Above we defined the pressure  $p$  as a force  $F$  per unit area  $A$ . Let us now have a closer look at how a pressure is created in a gas atmosphere and on a solid surface in contact with the gas, respectively. By doing so, we will also shed light on other phenomena occurring in a gas atmosphere. The kinetic theory of gases provides us with a description of the interactions between molecules of an ideal gas [1]. Such an ideal gas is a reasonable approximation of a real gas, particularly at extreme dilution or high temperature. We will have a closer look at real gas properties in Sect. 2.2.2. In an ideal gas, there are no attractive or repulsive forces between gas molecules [13]. The gas molecules behave like independent elastic spheres, with average distances between adjacent molecules that are large compared to the molecules' diameters.

The basics of the kinetic gas theory are as follows: gas consists of a large number of gas particles [1, 20]. A cubic meter of gas at a temperature of 23 °C and at a pressure of  $10^5$  Pa (atmospheric pressure) contains  $2.84 \times 10^{25}$  molecules, while a reduction of the pressure to  $10^{-7}$  Pa ( $7.5 \times 10^{-10}$  Torr—ultrahigh vacuum range) at otherwise identical conditions results in  $2.5 \times 10^{13}$  molecules.

The gas molecules are in a continuous state of random motion without any preference in direction. Each molecule moves along a straight line, until it collides with another molecule or the wall of the pressure vessel. Due to the impact, it changes its direction and continues on another straight path in another direction, and so on (Fig. 2.5). The distance between two respective collisions is called “free path”  $\lambda$ , while the average distance is related to as “mean free path”  $\lambda_{mfp}$ .

In the ideal gas, the gas molecules do not exert forces onto each other except for collisions (i.e., the moment of contact). Collisions of gas molecules with each other and with the wall are elastic. The impact due to collisions with the wall generates the gas pressure.

**Fig. 2.5** Free path  $\lambda$  of gas particles between collisions

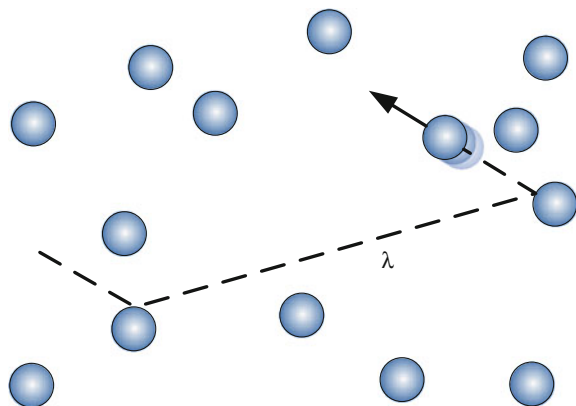
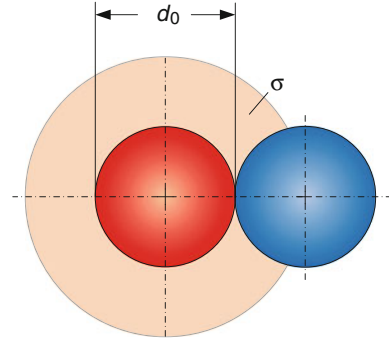




**Fig. 2.6** Atom diameter  $d_0$  and scattering cross section  $\sigma$



### 2.2.1.1 Mean Free Path

The mean free path  $\lambda_{mfp}$  depends on the scattering cross section  $\sigma = \pi d_0^2$  which depends on the diameter  $d_0$  of the gas molecules (Fig. 2.6) and the gas density  $n$  in molecules per cubic meter. The following equation describes the mean free path [1]:

$$\lambda_{mfp} = \frac{1}{\sqrt{2}\pi d_0^2 n}. \quad (2.12)$$

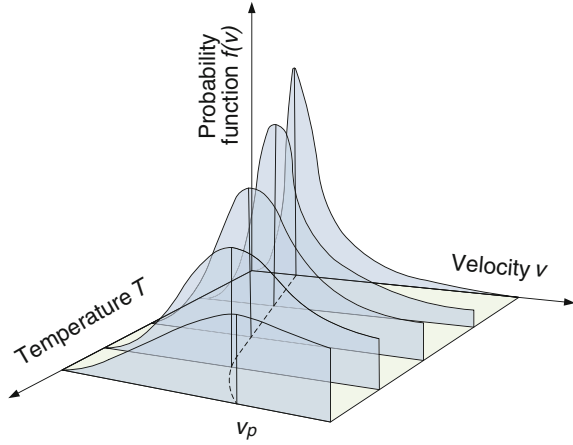
### 2.2.1.2 Velocity Distribution

The continuous elastic collisions and the accompanying exchange of kinetic energy result in a distribution of the gas molecules' velocities. The Maxwell–Boltzmann equation gives the probability distribution  $f(v)$  of the particle velocities [13]

$$f(v) = \frac{1}{n} \frac{dn}{dv} = \frac{4}{\sqrt{\pi}} \left( \frac{M}{2RT} \right)^{\frac{3}{2}} v^2 \exp\left(-\frac{Mv^2}{2RT}\right), \quad (2.13)$$

where  $n$  is the total number of molecules,  $M$  the molecule's molecular weight,  $R$  the gas constant, and  $T(K)$  the molecule's absolute temperature. The function is zero for both zero and infinite velocities. Figure 2.7 provides a three-dimensional representation of the Maxwell–Boltzmann equation. It shows a family of curves for the velocity probability distribution  $f(v)$  as a function of velocity  $v$  for various temperatures  $T$ . What is not obvious from Fig. 2.7 is that the velocity probability distribution also depends on the particle's molecular mass.

**Fig. 2.7** Velocity probability (Maxwell-Boltzmann) function  $f(v)$  for various temperatures  $T$ . It also shows the most probable velocity  $v_p$



The equation for only one component direction is as follows (taking the  $x$ -direction as an example):

$$f(v_x) = \frac{1}{n} \frac{dn}{dv_x} = \sqrt{\frac{M}{2\pi RT}} \exp\left(-\frac{Mv_x^2}{2RT}\right). \quad (2.14)$$

Equations (2.13) and (2.14) allow us to derive characteristic velocities, like the most probable velocity  $v_p$  (which occurs at the peak of each curve for  $dN/dv$ , see Fig. 2.7)

$$v_p = \sqrt{\frac{2RT}{M}}, \quad (2.15)$$

the arithmetic mean velocity  $\bar{v}$  which is important for calculations of the particle flow

$$\bar{v} = \frac{\int_0^\infty v \frac{dN}{dv} dv}{\int_0^\infty \frac{dN}{dv} dv} = \sqrt{\frac{8RT}{\pi M}}, \quad (2.16)$$

the mean square velocity  $\bar{v}^2$ , and the mean root square velocity  $\sqrt{\bar{v}^2}$ , respectively:

$$\bar{v}^2 = \frac{\int_0^\infty v^2 \frac{dN}{dv} dv}{\int_0^\infty \frac{dN}{dv} dv} = \frac{3RT}{M} \quad (2.17)$$

$$\sqrt{\bar{v}^2} = \sqrt{\frac{3RT}{M}} \quad (2.18)$$

As an example, let us calculate the arithmetic mean velocity  $\bar{v}$  of air at 27 °C. We will carry the dimensions, which is a good engineering practice for thermodynamic calculations. It will alert us to errors, if the unit for the value we are calculating is incorrect (e.g., anything but m/s for a velocity).

Starting point is Eq. (2.16):

$$\bar{v} = \sqrt{\frac{8RT}{\pi M}}.$$

Constants and values required are:

$$\begin{aligned} R & 8.314 \frac{\text{kJ}}{\text{K kmol}} \\ T & 27 \text{ }^\circ\text{C} \text{ (equals } 300.15 \text{ K)} \\ M_{\text{air}} & 28.89 \frac{\text{kg}}{\text{kmol}}. \end{aligned}$$

We further need the relationship between the dimensions for force [N], acceleration [m/s<sup>2</sup>], and mass [kg], which follows Newton's Law:

$$1 \text{ N} = 1 \text{ kg} \frac{\text{m}}{\text{s}^2} \quad (2.19)$$

$$\bar{v} = \sqrt{\frac{8 \cdot 8.314 \text{ kJ} \cdot 300 \text{ K kmol}}{\pi \text{ K kmol}} \frac{\text{kNm}}{28.89 \text{ kg}} \frac{\text{kg m } 10^3 \text{ N}}{\text{kJ}} \frac{\text{N}}{\text{Ns}^2} \frac{\text{N}}{\text{kN}}} \quad (2.20)$$

$$\bar{v} = 468 \frac{\text{m}}{\text{s}} = 1,695 \frac{\text{km}}{\text{h}}. \quad (2.21)$$

For comparison, let us calculate  $v_p$  and  $\sqrt{\bar{v}^2}$ . Dividing Eq. (2.16) by (2.15) and (2.18), respectively, gives:

$$v_p = \frac{1}{2} \sqrt{\pi \bar{v}} = 414 \frac{\text{m}}{\text{s}} = 1,502 \frac{\text{km}}{\text{h}} \quad (2.22)$$

$$\sqrt{\bar{v}^2} = \sqrt{\frac{2}{3}} \bar{v} = 382 \frac{\text{m}}{\text{s}} = 1,384 \frac{\text{km}}{\text{h}}. \quad (2.23)$$

### 2.2.1.3 Pressure Creation

By now we have seen that the gas molecules traveling with a velocity  $v$  impinge on the surface of the container wall [13]. It is the momentum transfer from these gas

molecules that causes the pressure  $p$  on a surface. The kinetic theory for ideal gases allows us to calculate the pressure:

$$p = \frac{1}{3} \frac{nM}{N_A} \bar{v}^2 = \frac{nRT}{N_A}. \quad (2.24)$$

$N_A$  is Avogadro's number,  $M$  the molar weight of the gas molecules, and  $n/N_A$  the number of mole per unit volume.

#### 2.2.1.4 Surface Impingement Rate

After discussing the interaction of gas molecules with a surface causing pressure, let us now have a look at the flow  $\Phi_c$  [molecules/m<sup>2</sup>-s or molecules/cm<sup>2</sup>-s] of contaminant gas molecules impinging on the container wall [13].  $\Phi_c$  is the surface impingement rate, the number of molecules per unit area and per second with a velocity component  $v_x$ , perpendicular to the wall surface:

$$\Phi_c = \int_0^{\infty} v_x dv_x. \quad (2.25)$$

Substitution of (2.14) gives

$$\Phi_c = n \sqrt{\frac{M}{2\pi RT}} \cdot \int_0^{\infty} v_x \exp\left(-\frac{Mv_x^2}{2RT}\right) dv_x = n \sqrt{\frac{M}{2\pi RT}}. \quad (2.26)$$

Substitution of Eq. (2.16) results in

$$\Phi_c = \frac{N_A p}{\sqrt{2\pi MRT}}. \quad (2.27)$$

#### 2.2.1.5 Monolayer Formation Time

For both thin-film processes and thin-film analysis, it is of interest how quickly the ambient atmosphere results in a contamination of a probe. Of particular interest is how long it takes for a monolayer contamination film to form. The monolayer formation time is gained by inverting the equation for the flow  $\Phi$ . Assuming that all gas molecules impinging on the surface are trapped, the formation time  $t_c$  for a monolayer contamination film is as follows:

$$t_c = \frac{n_{mono}}{\Phi} = \frac{n_{mono}}{N_A p} \sqrt{2\pi MRT}, \quad (2.28)$$

where  $n_{mono}$  is the number of molecules per unit area. For real applications, only a certain percentage of the incoming gas molecules sticks to the surface. A sticking coefficient expresses the probability of an impinging gas molecule to adhere to the surface or not. Particularly for chemical reactions between incoming atom and the surface, the sticking coefficient approaches 1. An example for such a strong interaction is  $O_2$  or  $H_2$  molecules reacting with a clean Si wafer surface. If there is no chemical reaction and there are only weak bonds forming, the sticking coefficient is much smaller, e.g., for some gases interacting with a graphite surface, the sticking coefficient is close to 0.

Let us now calculate  $t_c$  for  $10^5$  Pa (750 Torr), as well as  $10^{-6}$  Pa ( $7.5 \times 10^{-9}$  Torr). For a surface layer, the required number  $n_{mono}$  is approx.  $10^{15}$  gas molecules/cm<sup>2</sup> [13] or  $10^{19}$  gas molecules/m<sup>2</sup>. In a first step, we are substituting all constants in Eq. (2.28) and are expressing  $t_c$  as a function of the variables' molecular weight  $M$ , expressed in kg/kmol, temperature  $T$  in K, and pressure  $P$  in Pa. The constants are:

$$N_A: 6.022 \times 10^{26} \text{ kmol}^{-1}.$$

(Note: in this case Avogadro's number per kmol, not per mol).

$$R: 8.314 \frac{\text{kJ}}{\text{K kmol}}.$$

We also need the following relationships (see Eq. (2.19)):

$$\begin{aligned} 1 \text{ N} &= 1 \text{ kg} \frac{\text{m}}{\text{s}^2} \\ 1 \text{ kJ} &= 10^3 \text{ Nm} \end{aligned} \quad (2.29)$$

$$t_c = \frac{10^{19} \text{ m}^2}{\left(\frac{p}{\text{Pa}}\right) \text{ N}} \frac{\text{kmol}}{6.02 \times 10^{26}} \sqrt{2\pi \left(\frac{M}{\text{kg/kmol}}\right) \frac{\text{kg}}{\text{kmol}} \frac{\text{Ns}^2}{\text{kg m}} \frac{8.314 \text{ kJ } 10^3 \text{ Nm}}{\text{K kmol kJ}} \left(\frac{T}{\text{K}}\right) \text{ K s}} \quad (2.30)$$

$$t_c = 7.263 \times 10^{-11} \frac{\sqrt{\left(\frac{M}{[\text{kg/kmol}]}\right) \left(\frac{T}{[\text{K}]}\right)}}{\left(\frac{P}{[\text{Pa}]}\right)} [\text{s}]. \quad (2.31)$$

Next, we are substituting the molecular mass of air and 22 °C as its temperature, but are still keeping pressure  $p$  as a parameter:

$$T \quad 22 \text{ °C (equals approx. 295 K)}$$

$$M_{air} \quad 28.99 \frac{\text{kg}}{\text{kmol}}.$$

$$t_c = \frac{350.92 \times 10^{-6}}{\left(\frac{P}{[\text{Pa}]}\right)} [\text{s}]. \quad (2.32)$$

For our pressures originally chosen, the results for the contamination times are as follows:

$$t_c(10^5 \text{ Pa}) = 3.5 \cdot 10^{-9} \text{ s} = 3.5 \text{ ns}$$

$$t_c(10^{-6} \text{ Pa}) = 350 \text{ s} = 9.7 \text{ min.}$$

Figure 2.8 presents an overview over various parameters we discussed so far. It shows the molecular density, incident rate, mean free path, and monolayer formation time as a function of the system pressure. Particularly, the monolayer formation time, ranging from nanoseconds to a year depending on the quality of the technical vacuum, highlights the need for vacuum conditions for many deposition techniques.

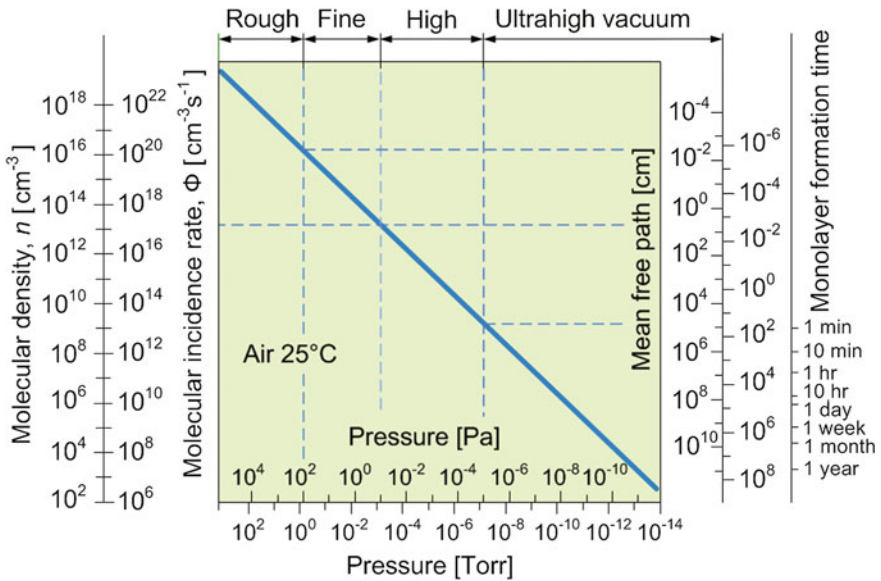


**Fig. 2.8** Molecular density, incident rate, mean free path, and monolayer formation time as a function of pressure. *Source* Ohring [13]. Used with permission

### 2.2.2 Ideal and Real Gas

The equations presented so far were for ideal gases. The differences between an ideal gas and a real gas are that (i) the ideal gas has gas molecules with a volume equal zero (point-like masses), (ii) there are no interactive forces between the gas molecules, and the gas molecules are single atom molecules [21]. In reality, the gas molecules do have a volume, which results in a space not available for gas molecules to travel to. In real gases, this volume is taken into account as “co-volume.” Furthermore, there is an attraction between the gas molecules due to van der Waals forces. These forces result in an internal pressure, which affects the scattering cross section of the gas molecules.

For a derivation, we start with the expression for the ideal gas given in Eq. (2.6)

$$pV = \frac{m}{M}RT, \quad (2.33)$$

where  $p$  is the pressure, the ratio  $m/M$  describes the number of moles present in volume  $V$ ,  $R$  is the gas constant, and  $T$  the absolute temperature. Augmenting the ideal gas equation by respective terms for internal pressure and co-volume results in the van der Waals equation for real gases [21, 22]:

$$\left(p_{real} + \frac{n^2a}{V^2}\right)(V - nb) = \frac{m}{M}RT \quad (2.34)$$

$$\left(p_{real} + \frac{n^2a}{V^2}\right) = p_{eff} \quad (2.35)$$

$$(V_{real} - nb) = V_{eff} \quad (2.36)$$

$a$  and  $b$  are van der Waals constants,  $p_{eff}$  is the effective pressure, and  $V_{eff}$  the effective volume.

As mentioned before, real gases behave like ideal gases at low concentrations and at high temperatures. Equation (2.34) demonstrates why: because large volumes contain only small numbers of gas molecules therefore, the volume of the molecules itself is only a small fraction. Likewise, the molecules' attractive forces are very small compared to the impact forces. As a result, the increase in the scattering cross section is also small.

## 2.3 Gas Flow

### 2.3.1 Flow Regimes

Gas flow is needed to reduce pressure in systems (vacuum chamber, pipe). The pressure in the vacuum chamber during pump-down passes through up to 13 orders of magnitude (see Table 2.1), with the number of gas molecules per  $\text{m}^3$  reduced from  $2.7 \times 10^{25}$  at  $10^5$  Pa (atmospheric pressure) to  $2.7 \times 10^{12}$  at  $10^{-8}$  Pa (ultrahigh vacuum). The various gas flow conditions are a function of system dimension and pressure [13]. Figure 2.9 illustrates the dominant gas flow regimes as a function of system dimensions and pressure. At one end, close to atmospheric pressure, there is a viscous flow regime. At the other end, at ultrahigh vacuum pressures, we find free molecular flow. In between, there is a transition area.

To quantitatively characterize gas flow regimes, one uses dimensionless numbers such as the Knudsen and the Reynolds numbers. They are related to the ratio of pressure and volume.

Knudsen number  $\text{Kn}$  is the quotient of the mean free path  $\lambda_{mfp}$  and the pipe diameter  $d$  [1, 13]. The mean free path is related to the pressure but also comprises

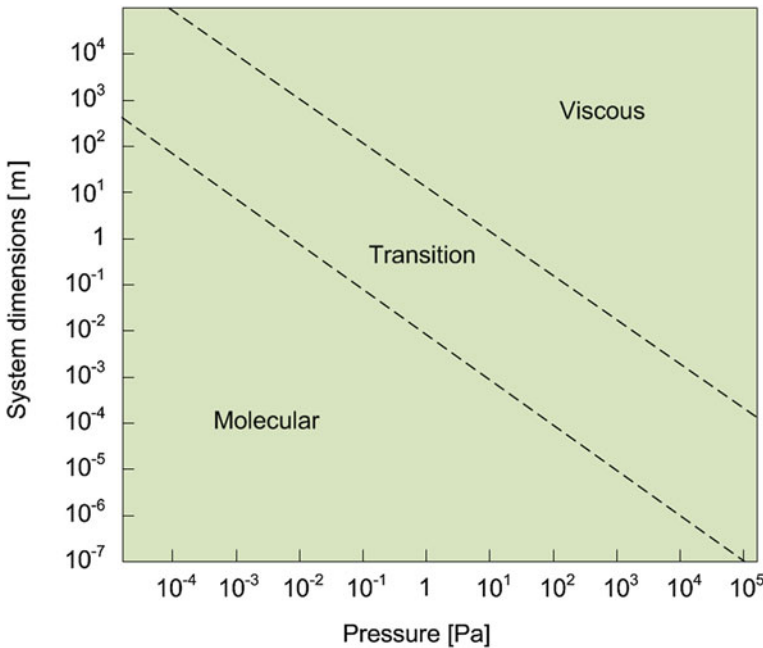


**Fig. 2.9** Dominant gas flow regimes as a function of system dimensions and pressure. *Source* Ohring [13]. Used with permission



**Table 2.2** Flow regimes and knudsen numbers

Flow regime	Knudsen Number
Viscous flow	$\text{Kn} < 0.01$
Intermediate flow	$1 > \text{Kn} > 0.01$
Molecular flow	$\text{Kn} > 1$

Source O'Hanlon [1]

the nature of the gas as the molecules scattering cross section is taken into account as well

$$\text{Kn} = \frac{\lambda_{mfp}}{d}. \quad (2.37)$$

Table 2.2 illustrates Knudsen numbers for the flow range shown in Fig. 2.9. Within the different flow regimes, alternative working principles for pumping as well as for pressure measurement are needed.

The Reynolds number  $\text{Re}$  characterizes the air flow in a pipe (laminar or turbulent) [1]. The Reynolds number  $\text{Re}$  for round pipes is [1]

$$\text{Re} = \frac{u\rho d}{\eta}, \quad (2.38)$$

where  $u$  [m/s] is the stream velocity,  $\rho$  [kg/m<sup>3</sup>] the mass density of the gas,  $d$  [m] the pipe diameter, and  $\eta$  [Ns/m<sup>2</sup> = kg/m-s] the dynamic viscosity, which is a measure of the internal resistance.

### 2.3.2 Viscous Flow

Ideally, the flow in pipes of low and medium vacuum systems is viscous and laminar [1]. At a wall there is no gas velocity due to the formation of a boundary layer. Viscous flow occurs for Knudsen numbers below 0.01 and Reynolds numbers below 1,200.

### 2.3.3 Molecular Flow and Transition Regime

A molecular flow is considered to start when the mean free path exceeds the pipe diameter (this corresponds to a Knudsen number  $> 1$  [1]). In this regime, viscosity is no longer found and collisions between gas molecules and pipe or vacuum chamber wall predominate. Most probable are diffuse reflections: the incident gas molecule sticks to the surface, moves back and forth in a surface imperfection, and is re-emitted, leaving the surface in a random direction [1].

In a transition regime with  $1 > \text{Kn} > 0.01$ , the gas flow is neither viscous nor molecular. The pipe diameter has a dimension of several mean free paths  $\lambda_{\text{mfp}}$ . Contrary to the viscous flow, the velocity is not zero at the wall. A theoretical approach to treat this range is difficult [1].

## 2.4 Vacuum Systems—Overview

A vacuum system typically consists of a vacuum chamber, which serves as a pressure vessel to allow a vacuum at its inside and a pump system to create the vacuum. Frequently, the vacuum chamber is also called a recipient. Inside the vacuum chamber are the fabrication or analysis equipment components requiring a vacuum environment, as well as the fabrication or analysis samples (e.g., substrates).

### 2.4.1 Vacuum Chamber

Figure 2.10 provides a schematic representation of a vacuum chamber for a production or analysis tool. Such systems, independently of their use in wafer fabrication (deposition, etching, analysis, etc.); typically contain a substrate table on which the substrates are positioned during processing or analysis. Such a vacuum

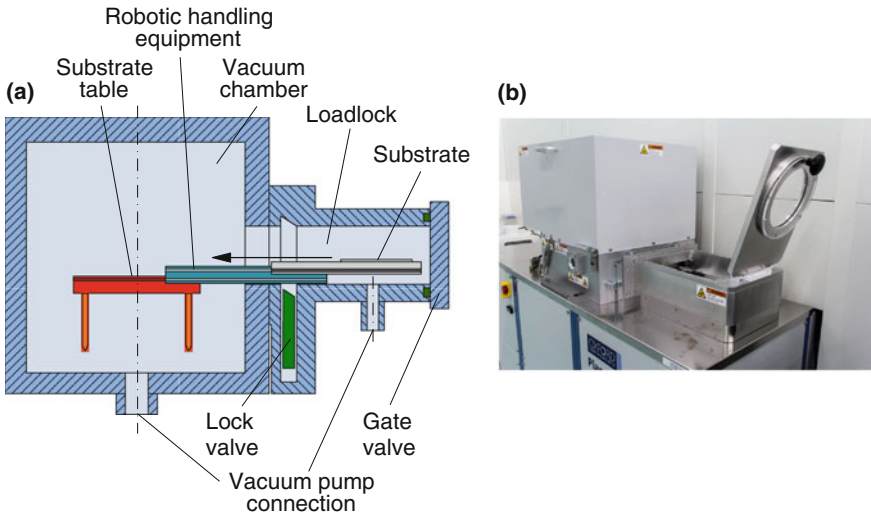


**Fig. 2.10** Loadlock. **a** Schematic representation of a loadlock (frontloaded). **b** Loadlock (toploaded) of a dry etching system (ICP-DRIE, see Chap. 4). *Photograph: IMPT, Leibniz Universität Hannover*

chamber may be opened directly to load and unload the substrates. To avoid a total flooding with air during such a process, the vacuum chamber may be equipped with a loadlock, as shown in Fig. 2.10. This way only the loadlock is flooded. The loadlock may have a connection to the vacuum pump system on its own. This way penetration of air and in particular moisture into the vacuum chamber is minimized. Robotic handling equipment transports the substrate between loadlock and vacuum chamber.

A loadlock takes on an additional function if used in conjunction with a cluster tool, i.e., a combination of at least two fabrication tools. In such a case, it not only allows to load and unload substrates, it also shuttles substrates from one of the cluster's tool to another without exposing them to atmospheric pressure (and thus contamination). Such a system is called a transport module.

### **2.4.2 Pumps**

The vacuum pump system evacuates the vacuum chamber. In case that a high vacuum or an ultrahigh vacuum has to be achieved the pump system first operates in the viscous regime, then in the transition regime, and at the end in the molecular regime. There is no single vacuum pump that is capable of operating in all regimes alike. Therefore, a system working in the high or ultrahigh vacuum range typically consists of two pumps, a roughing pump and a high vacuum pump. Typically, the connection between the two types of pumps is called a foreline and the operating pressure in it fore-vacuum.

#### **2.4.2.1 Roughing Pump**

A roughing pump is any pump that removes the bulk of the gas molecules in the rough vacuum range and its viscous flow regime, reaching fore-vacuum conditions sufficient for a high vacuum pump starting its operation. Typically, a mechanical pump capable of working against atmospheric pressure performs this task. Oil-sealed or dry roughing pumps are utilized. For oil-sealed roughing pumps, the oil used not only for sealing, but also for lubrication is exposed to the vacuum and may result in hydrocarbon backstreaming, which may be detrimental to some fabrication processes.

#### **2.4.2.2 High Vacuum Pump**

A high vacuum pump is any pump capable of reaching very low pressure ( $<10^{-1}$  Pa /  $7.5 \times 10^{-4}$  Torr—high vacuum or better) by pumping in the transition and molecular range. These pumps are not capable of operating in the low-vacuum range—at least not efficiently. In a vacuum pump process, they start their operation as soon as the

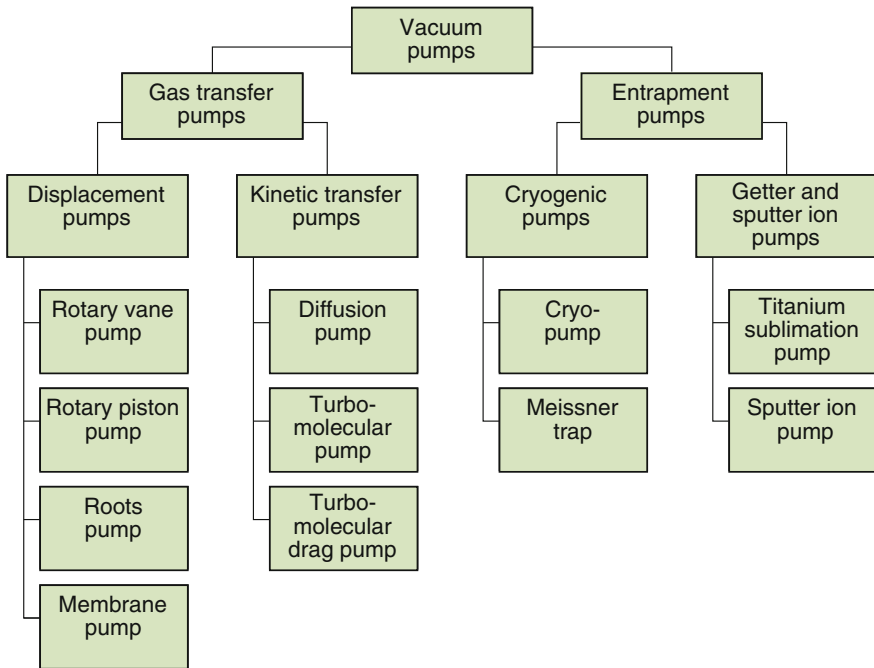


**Fig. 2.11** Overview over vacuum pumps

roughing pump has lowered the pressure in the vacuum chamber to fore-vacuum in the rough or medium vacuum range.

### 2.4.2.3 Vacuum Pump Principles

Besides differentiating pumps by the pressure they reach (roughing pumps and high vacuum pumps), they may also be classified by their operation principle into gas transfer pumps and entrapment pumps [1, 2]. Figure 2.11 presents an overview. Gas transfer pumps remove gas molecules by transport from the vacuum chamber in one or more steps of compression. Gas transfer pumps may be designed as positive displacement pumps or kinetic transfer pumps. In contrast to gas transfer pumps which remove gas permanently, entrapment pumps capture the gas molecules in a solid or adsorbed state inside the vacuum chamber. Some of the entrapment pumps may be operated reversibly during a regeneration cycle, releasing trapped or condensed gas back into the system.

Examples of positive displacement pumps are the rotary vane pump, piston pump, lobe (Roots) pump, and diaphragm pump. All four are applied as roughing pumps in vacuum systems. Examples of kinetic transfer pumps are the diffusion pump and the turbomolecular pump with and without drag stage. All are high and ultrahigh vacuum pumps. Examples of entrapment pumps are the cryopump,

Meissner trap, titanium sublimation pump, and sputter ion pump. With the exception of the cryopump, they are auxiliary pumps boosting high vacuum performance. All of these vacuum pumps will be discussed in greater detail below.

## 2.5 Roughing Pumps

### 2.5.1 Rotary Vane Pump

The rotary vane pump is an oil-sealed pump. Figure 2.12 presents the pump and its operating cycle. Figure 2.12a schematically shows the pump and its components. The contact area between vane and suction chamber wall forms a seal due to spring and centrifugal load on the vane, as well as a low vapor pressure fluid, which also serves as a lubricant.

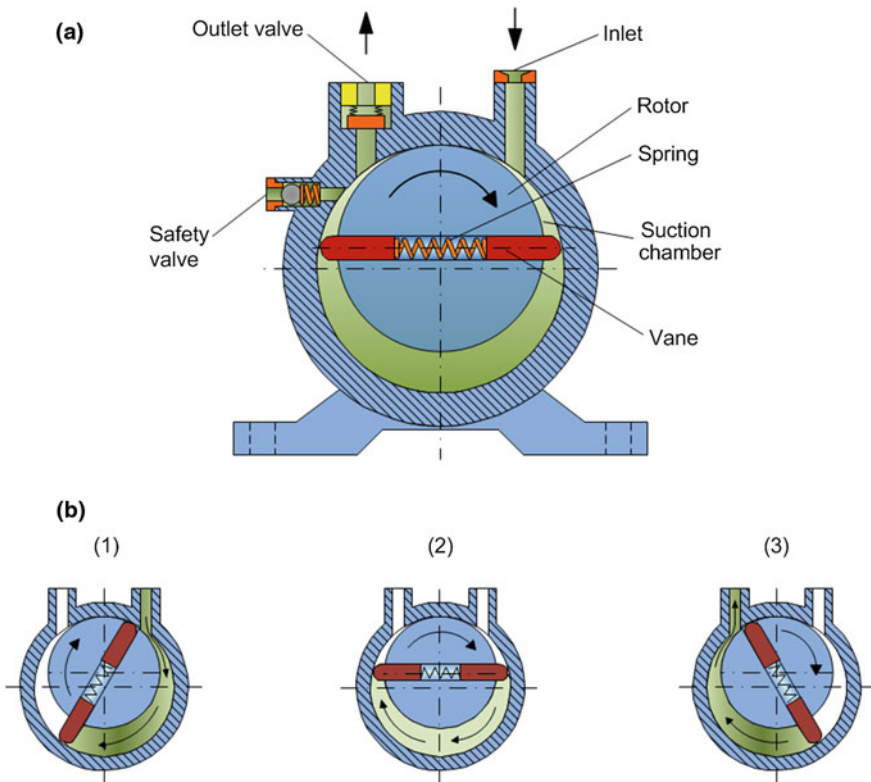


**Fig. 2.12** Rotary vane pump (adapted from Umrath [2]). **a** Pump components. **b** Pumping sequence

The operation sequence is as follows (Fig. 2.12b) [1]: Gas to be pumped enters the suction chamber through an inlet (phase 1). The inlet is connected to the exhaust of the high vacuum pump by a foreline. The gas is compressed by rotor and vane (phase 2) and expelled through an exhaust (outlet) valve (phase 3). The pump performs two pumping cycles per revolution. The system shown features a safety valve which prevents damage to the pump in case the discharge flow beyond the exhaust valve is blocked.

If corrosive gases are pumped, special corrosion resistant vacuum oils have to be used. A widely applied lubricant for such applications is Fomblin<sup>®</sup>, a perfluoropolyester (PFPE).

The rotary vane pump is capable of pumping gas in a pressure range of 1–10<sup>5</sup> Pa ( $7.5 \times 10^{-3}$ –750 Torr) [1]. It is the most commonly used roughing pump for small and mid-size vacuum systems. For this application, its pumping speed (or pumping rate) is 10–200 m<sup>3</sup>/h.

### 2.5.2 Rotary Piston Pump

Like the rotary vane pump, the rotary piston pump (also called rotary plunger pump), is an oil-sealed roughing pump. The working principle is similar to the one of a rotary vane pump, except that, instead by a vane, a cylindrical piston facilitates the periodic change of the suction chamber's size. Figure 2.13 depicts a schematic representation of a rotary piston pump and its operating cycle [1, 2]. Figure 2.13a shows the pump and its components. The piston, driven by an eccentric, moves along with the chamber wall. Figure 2.13b demonstrates three steps of the two rotation operating cycles. The gas to be pumped flows from the inlet through a channel and slit of the hinge bar into the pumping chamber. At 180° rotation, the pump is in the middle of its suction cycle. After one revolution (360°), the chamber volume is at a maximum, and the slit is closed, completely isolating the gas volume from the inlet. During the next revolution, the gas is compressed and leaves the pump through an oil-sealed poppet valve. At 540°, the pump is in the middle of its compression and exhaust cycle.

Pumping corrosive gases requires the same precautions as taken with a rotary vane pump. Fomblin<sup>®</sup> as a lubricant can also be utilized in a rotary piston pump.

The rotary piston pump is capable of pumping gas in a pressure range of 1–10<sup>5</sup> Pa ( $7.5 \times 10^{-3}$ –750 Torr) [1]. Typical rotational velocities are between 400 and 600 min<sup>-1</sup>. The pumping speed is 30–1,500 m<sup>3</sup>/h.

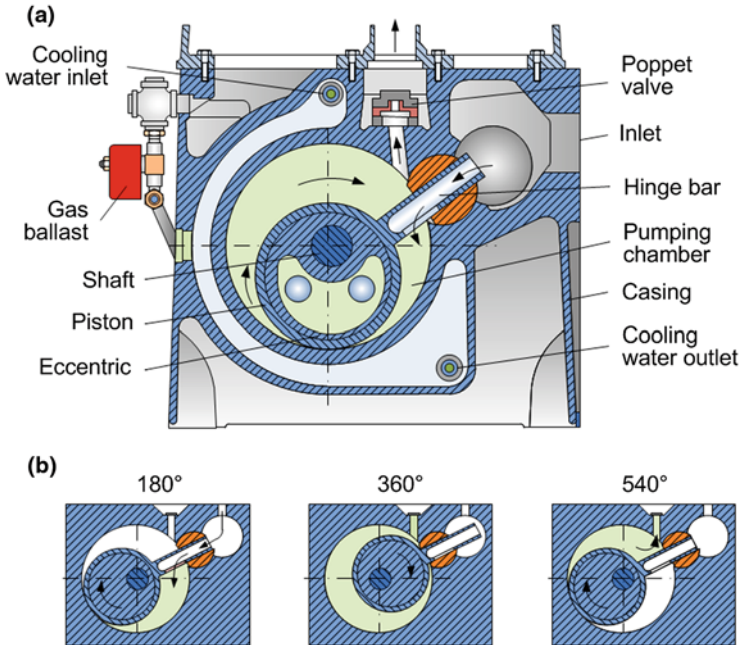
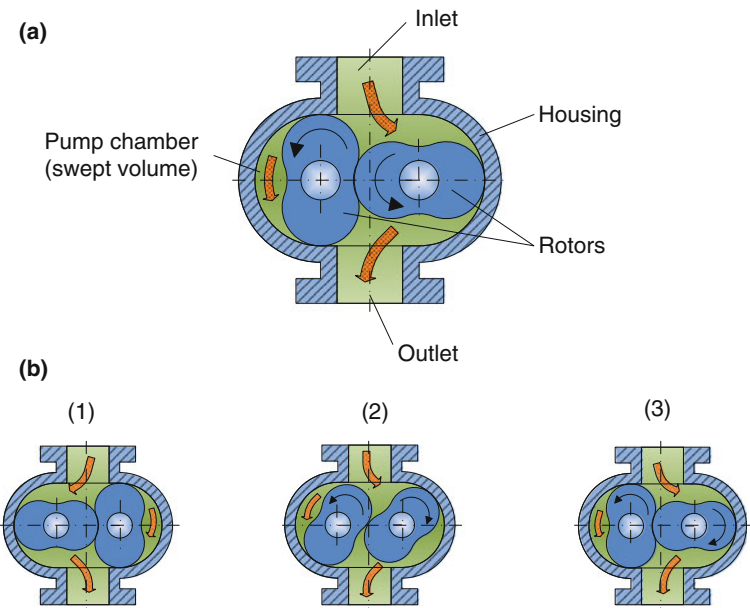


**Fig. 2.13** Rotary piston pump. **a** Pump components (adapted from Ohring [13]). **b** Pumping sequence (adapted from Umrath [2])

### 2.5.3 Roots Pump

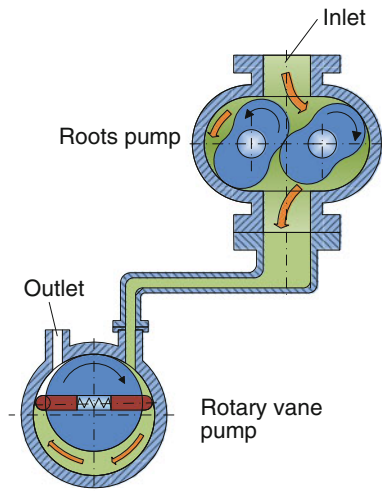
The lobe blower, better known as Roots pump, is used in series with a rotary vane or piston pump. An isolated use of a Roots pump as a roughing pump is not possible, because this type of pump is unable to work against atmospheric pressure. The reason is found in its design: Roots pumps feature two figure eight-shaped rotors mounted on parallel shafts and are rotating in opposite direction (Fig. 2.14). There is a substantial clearance both between the rotors themselves as well as between each rotor and the housing. Due to this clearance—typically about 0.2 mm—the rotors operate at a rather high rotational velocity of 3,000–3,500  $\text{min}^{-1}$  and do not require lubrication. While Fig. 2.14a schematically shows the pump and its components, Fig. 2.14b illustrates its operating cycle.

Figure 2.15 demonstrates the combination of a rotary vane and a Roots pump. Such a combination substantially boosts pumping speed and increases the achievable vacuum range. As an example, by combining a rotary piston pump with a Roots pump, the pumping speed can be roughly increased from 100 to 450  $\text{m}^3/\text{h}$  [1].



**Fig. 2.14** Roots pump (adapted from Umrath [2]). **a** Pump components. **b** Pumping sequence

**Fig. 2.15** Combination rotary vane/Roots pump



### 2.5.4 Diaphragm Pump

The main advantage of a diaphragm pump is its oil-free operation. Therefore, it is the ideal pump for applications that do not tolerate hydrocarbon backstreaming. They do have a major drawback: the attainable fore-vacuum pressure is only 7,000–20,000 Pa



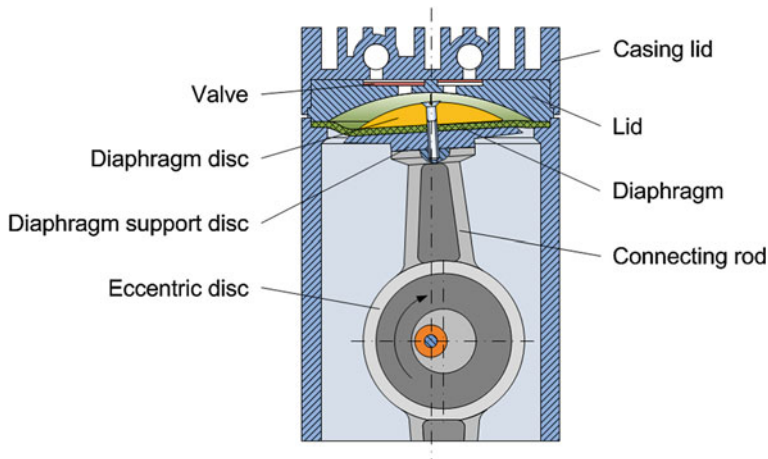


**Fig. 2.16** Diaphragm pump (adapted from Umrath [2])

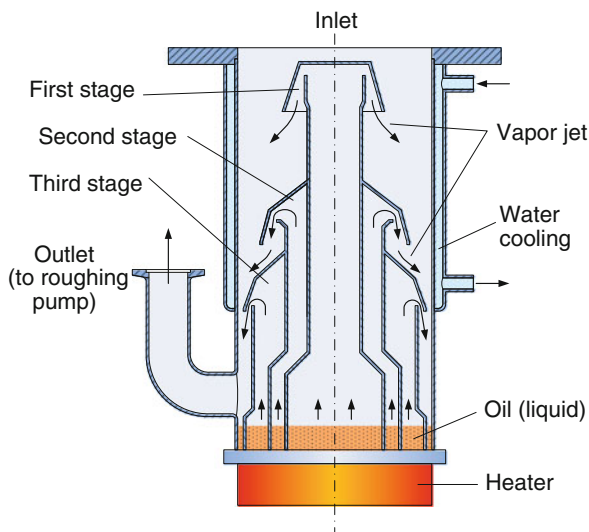
(50–150 Torr) for single-stage pumps and 700–1,400 Pa (5–10 Torr) for dual-stage pumps [1].

Figure 2.16 schematically shows a diaphragm pump [2]. A diaphragm is mounted between pump head and casing with its circumference tensioned. Driven by an eccentric drive and a connecting rod, its center performs an oscillatory motion. Due to this motion, the volume of the compression chamber above the diaphragm changes periodically. During expansion, an inlet valve opens and the gas to be pumped flows into the compression chamber. During compression, the inlet valve closes and the gas leaves the compression chamber through the outlet valve. Neither the diaphragm nor the valves require the use of sealing oil. The pump is capable of pumping corrosive gases.

Besides being an oil-free pump, other advantages of a diaphragm pump are high durability, easy exchange of the diaphragm and valves, low sound emission, and a compact design. However, the low attainable pressure requires the use of special high vacuum pumps, which are able comply with such a high starting pressure. We will see that there is one type of high vacuum pump, which can handle such operating condition: the turbomolecular drag pump (see Sect. 2.6.3).

## 2.6 High Vacuum Pumps I—Kinetic Transfer Pumps

As already mentioned, a high vacuum pump is any pump capable of reaching high vacuum or better ( $<10^{-1}$  Pa ( $7.5 \times 10^{-4}$  Torr)). Therefore, for matters of simplicity, pumps reaching the ultrahigh vacuum range are also referred to as high vacuum pumps.

**Fig. 2.17** Diffusion pump

### 2.6.1 Diffusion Pump

The name “diffusion pump,” originally coined by Gaede, in reality does not describe this pump appropriately, since the work principle is not diffusion [1]. Instead, the diffusion pump is a vapor jet pump: a high-speed vapor stream collides with the gas molecules; the pumping action is by momentum transfer upon impact. Most commonly, hydrocarbon oil is used as pumping fluid. A diffusion pump typically can pump to a pressure of  $5 \times 10^{-5}$  Pa ( $3.7 \times 10^{-7}$  Torr). The main advantage of a diffusion pump is its lack of any moving part.

Figure 2.17 provides a schematic representation of a diffusion pump [2]. The pump consists of a pump body with a cooled wall and a three (shown) or four stage nozzle system. The oil serving as pump fluid starts out its pumping cycle in a liquid state above an electric heater located at the bottom of the pump. Upon vaporization and superheating by the heater, the pump fluid vapor streams through the riser tube at one of the stages. The boiler pressure typically is 200 Pa (1.4 Torr). The oil vapor emerges with supersonic speed from ring-shaped Laval jet nozzles. The vapor jet, which widens after exiting, forms an umbrella of high-speed oil molecules. This momentum is transferred from the oil molecules of the pumping fluid to the gas molecules to be pumped. Upon reaching the wall, which is chilled by water-cooling, the pump fluid condenses. Back in a liquid state, the pumping fluid flows downwards on the pump’s sidewall as a thin film and finally returns to the heater. The gas molecules pumped gather below the lowest stage; from there, they are pumped off by the roughing pump. The latter is mandatory, since a diffusion pump cannot work against atmospheric pressure.

Due to potential chemical reactions, the use of hydrocarbons as pumping oil is prohibitive for pumping corrosive gases, as common in CVD processes.

Furthermore, any attempt to pump pure  $O_2$  would result in an explosion. A limited capability for pumping water vapor may be compensated by integrating a Meissner trap into the diffusion pump.

Backstreaming of oil into the vacuum chamber is a diffusion pump's most serious challenge [13]. For that reason, the use of diffusion pumps in the high-tech area is rather limited. However, other areas take advantage of vacuum technology by diffusion pumps. For instance, this is the case for the fabrication of decorative or optical coatings or coating tools.

### 2.6.2 Turbomolecular Pump

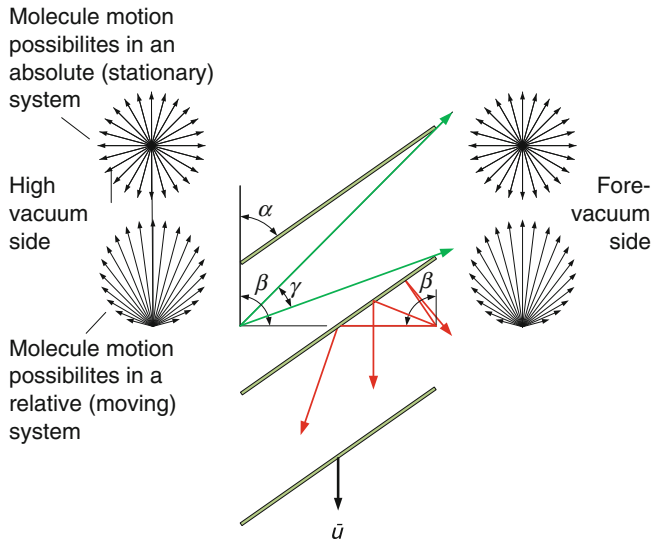
The turbomolecular pump compresses gas by transferring kinetic energy from high-speed rotating blades to gas molecules [1]. As already mentioned, the principle of the turbomolecular pumping was invented by Gaede in 1912. However, it was not until 1958 that a practical approach employing turbine blades was found and patented by Willi Becker, Arthur Pfeiffer Technik in Wetzlar, Germany (now Pfeiffer Vacuum) [23, 24].

Figure 2.18 presents an isometric view of a turbomolecular pump. The pump is an axial compressor. Its active part consists of a rotor and a stator. Both rotor and stator feature blades at their circumference. Each pair of rotor and stator rings represents one stage of the turbomolecular pump.

Due to rotor rotational velocities of  $24,000\text{--}80,000\text{ min}^{-1}$ , blade speeds are in the same range as the velocity of the gas molecules. This high blade velocity, in conjunction with the geometry of the moving rotor blades and stationary stator blades, create a geometry which favors a motion of the gas molecules from the

**Fig. 2.18** Turbomolecular pump. Courtesy of Oerlikon Leybold Vacuum





**Fig. 2.19** Travel of gas molecules through the turbomolecular pump blade geometry

pump inlet to the pump outlet, rather than the other way around. Figure 2.19 demonstrates why. The molecular velocity of the gas particles is in the same order of magnitude as the turbine velocity  $\vec{u}$ . In a system moving with this velocity  $\vec{u}$ , only molecule velocity vectors in the first two quadrants occur. This means, for molecules on the high vacuum side only vectors within the angle  $\beta$  (representing the first quadrant) move in the direction of the fore-vacuum. A molecule in the middle of the entrance of a channel formed by two adjacent blades (and tilted by an angle  $\alpha$ ) traveling with a velocity vector within the angle  $\gamma$  passes the slot without collision and enters the fore-vacuum side. Molecules on this fore-vacuum side are also able to only enter the turbine area within an angle of  $\beta$ , this time in the second quadrant. However, each motion in this direction results in scattering.

The gas to be pumped arrives directly (and therefore without loss of pressure) through the inlet flange at the first stage. Passing through all stages compresses the gas to fore-vacuum pressure. Typical compression rates are  $10^{10}$  for hydrocarbons,  $10^9$  for  $N_2$ , and  $10^3$  for  $H_2$  [13]. Contrary to a jet turbine fabrication, the rotor and all its blades is machined from one solid block of material. The rotor is mounted to a drive shaft, which typically is driven by a mid-frequency motor located in the part of the turbomolecular pump which is under fore-vacuum conditions, thus eliminating the need of a high vacuum feedthrough.

Due to the high rotational velocity, high-performance bearings are required. There are three alternatives for bearings in use [2]. The first one is oil-lubricated ball bearings with steel balls. They are low maintenance, but lend themselves only for a vertical installation. The second alternative is grease-lubricated hybrid bearings. They are lifetime-lubricated and may be installed in any direction. The third one is

bearings with magnetic levitation. They are wear-free and do not require maintenance. They are absolutely free of hydrocarbons and may be installed in any direction.

A special protection of the bearings is mandatory if a pumping of chlorinated and fluorine gases is required. This is the case for many deposition or etching processes (e.g., Plasma-enhanced Chemical Vapor Deposition—PECVD, see Sect. 3.5.7). Such gases cause corrosion on ball bearings or magnetic bearings. To avoid such corrosion, bearings are typically flooded with an inert gas (e.g.,  $N_2$ ). This way corrosive gases are kept out. With these precautions taken, the turbomolecular pump is the only high throughput high vacuum pump capable of pumping corrosive gases. Although turbomolecular pumps are rather expensive, they are increasingly employed for thin-film deposition and characterization equipments [13]. Typical ultimate pressures are  $10^{-8}$  Pa ( $7.5 \times 10^{-11}$  Torr) and typical pumping speeds  $50$ – $10^3$  l/s.

### 2.6.3 Turbomolecular Drag Pump

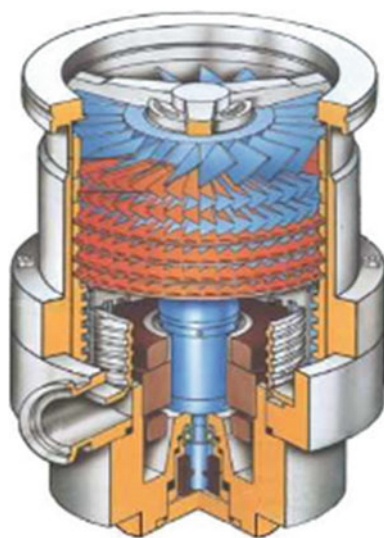
A magnetically levitated turbomolecular pump with a diaphragm roughing pump represents an oil-free system very attractive for applications sensitive to hydrocarbon contamination. However, the fore-vacuum pressure required by a turbomolecular pump is in the order of  $0.1$ – $1$  Pa ( $7.5 \times 10^{-4}$ – $7.5 \times 10^{-3}$  Torr) [1]. While oil-sealed rotary vane and rotary piston pumps are capable of reaching such a backing pressure, diaphragm pumps are not. For this reason, a molecular drag pump stage was incorporated on the axis of the turbomolecular pump at its high pressure end. The result is a turbomolecular drag pump.

The drag stage transports gas by means of high-speed molecular rotors. The rotor may either be a drum with helical grooves or a disc with spiral grooves. The drum shaped drag pump with helical grooves was invented by the French physicist Fernard Holweck (1890–1942) in 1923 [25]; the drag pump with a disc and a spiral groove was invented by Karl Manne Georg Siegbahn (1986–1978)<sup>2</sup> and first built in 1926 [27]. The compression rate of a drag stage depends on which type of gas is pumped and ranges from  $10^9$  for  $N_2$  to  $10^3$  for  $H_2$  [28]. Figure 2.20 presents a Holweck type turbomolecular drag pump [29]. It accepts a backing pump pressure of  $4$ – $20$  Pa ( $30$ – $150$  mTorr) and has a pumping speed similar to that of a conventional turbomolecular pump [1].

---

<sup>2</sup> Siegbahn was a Swedish Nobel laureate (Physics 1924, for his discoveries and research in the field of X-ray spectroscopy [26]).

**Fig. 2.20** Turbomolecular drag pump. Courtesy of Pfeiffer Vacuum [29]



## 2.7 High Vacuum Pumps II—Entrapment Pumps

### 2.7.1 Cryogenic Pumps I—Cryopump

A cryopump is a gas-entrapment pump that pumps by condensing gas molecules on chilled surfaces with a temperature below 120 K [1, 13]. Responsible for physically binding or adsorbing gas molecules are temperature dependent van der Waals or dispersion forces. Cryogenic pumps provide vacuum low in contamination at a pressure of  $10^{-1}$  to  $10^{-8}$  Pa ( $7.5 \times 10^{-4}$ – $7.5 \times 10^{-11}$  Torr). The cryopump itself is not a source of

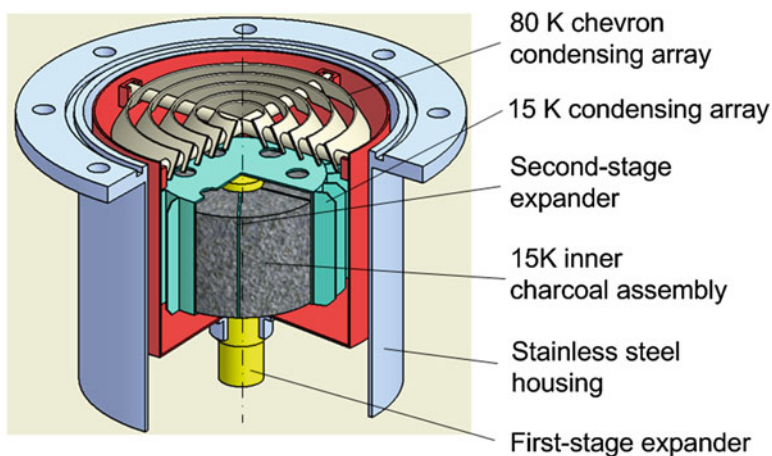


**Fig. 2.21** Cutaway view of a cryogenic pump

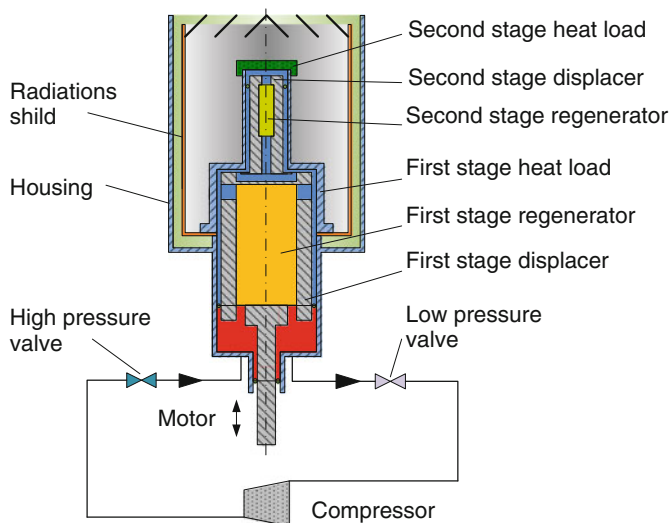


**Fig. 2.22** Schematic representation of a cryopump with a two-stage Gifford-McMahon helium gas refrigerator (adapted from Umrath [2])

contamination; the only contaminants found in the vacuum chamber are those not pumped. However, as an entrapment pump, it will ultimately be saturated [30].

Figure 2.21 presents a cutaway view of a cryopump [1, 2]. The pump has three different cooling surfaces, which jointly represent the cryopump's cold head. An 80 K condensing array is at the top of the pump inside the high vacuum flange, while the 15 K cooling area and an active charcoal is located beneath. The 80 K (first-stage) cooling area mainly condenses water, which accounts for the bulk of the gas load. Most of the remaining gases are condensing within the 15 K (second-stage) cooling area. However, there are exceptions: He,  $H_2$ , and Ne would require a third stage with a temperature of 4.2 K. This may not be accomplished with a reasonable effort. Instead, a portion of the 15 K cooling area is covered with activated charcoal to bind these gases by sorption.

The cryopump is a helium refrigerator with continuous flow using the Gifford-McMahon process [1, 2]. Figure 2.22 sketches a typical high vacuum cryopump array with a two-stage helium gas refrigerator. It consists of a remote compressor, two valves, and the cryopump itself with its two-stage cold head (also called expander) and cooling surfaces. The compressor and the cryopump are connected by flexible high pressure hoses to minimize the transmission of vibrations originating at the compressor.

The cooling action of a Gifford-McMahon gas refrigerator depends on the controlled expansion of He gas, involving transfer of energy from the warm incoming helium to the cold outgoing helium. It is accomplished in the cold head containing a two-stage displacer and two regenerators located inside of the displacers (the detailed cycle is described below). A radiation shield and a chevron condensing array are attached to the first (warm) stage of the cold head,

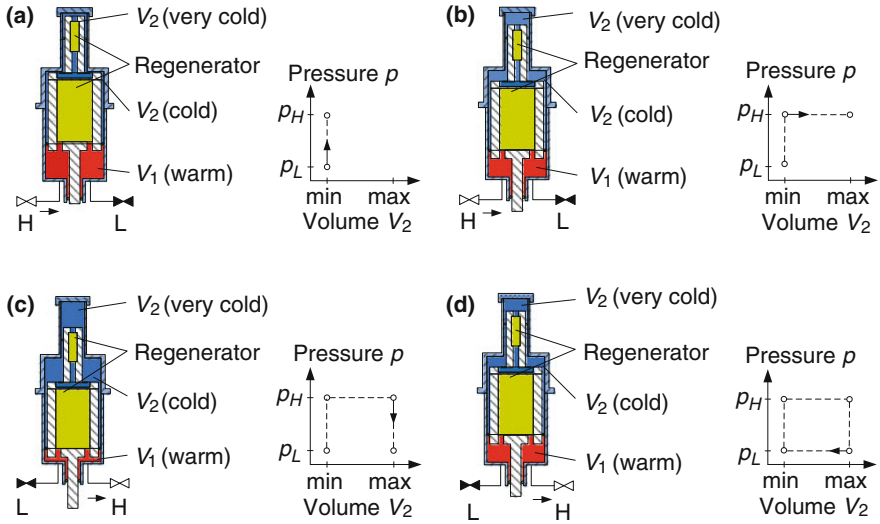


**Fig. 2.23** Cooling cycle of a two-stage Gifford-McMahon refrigerator (adapted from Umrath [2] and O'Hanlon [31]). For each phase, there is a picture presenting the respective displacer position, the state of the high and low pressure valve (open or closed), and a  $p$ - $V$  diagram showing the cyclic process state

representing the first-stage heat load. The inner pumping surface (second-stage heat load) is attached to the second (cold) stage.

Figure 2.23 allows us to have a look at a complete cycle of a two-stage Gifford-McMahon refrigerator.<sup>3</sup> For each phase, it shows (i) the displacer position, (ii) if the high and low pressure valve are open or closed, and (iii) a  $p$ - $V$  diagram for the cyclic process state.

At the beginning of a cycle (Fig. 2.23a), the two displacers are at their highest position in the cylinder. Through the open high pressure (inlet) valve, high pressure ambient temperature helium gas from the outlet of the compressor enters the regenerator; the low pressure (exhaust) valve is closed.

Next (Fig. 2.23b), while the high pressure valve is still open, the displacers move down, actuated by their drive motor. The incoming helium gas passes through the cold first-stage regenerator to the first-stage expansion chamber. A portion continues through the second-stage regenerator to the second-stage expansion chamber. The helium cools as it transfers heat to the respective regenerators. At this point in the cycle, the helium temperatures are about the same as the respective loads. Before the displacers reach the bottom of their strokes, the high pressure valve closes. Moving further, the displacers force the remaining helium gas through them.

With the displacers at the bottom of their strokes (Fig. 2.23c), the low pressure (exhaust) valve opens allowing the helium to expand. By expanding, the helium

<sup>3</sup> Adapted from O'Hanlon [31], who describes the Gifford-McMahon process for a single-stage helium gas refrigerator.



performs work; since no mechanical work is done, the expansion causes cooling. Heat flows from the loads and heats the helium up to a temperature somewhat below that at which it entered the lower cylinder area. As the gas flows upwards through the regenerator, it removes heat from it and cools it to the temperature at which it was found at the beginning of the cycle.

With the low pressure valve still open, the displacers are now moving upwards (Fig. 2.23d) to force the remaining helium gas from the end of the cylinder out through the regenerators and through the low pressure valve, cooling the regenerators while passing through. From there, the helium exhausts back to the compressor at ambient temperature. This concludes a cooling cycle.

As a result of the cooling, the temperature of the first (or warm) stage is 30–100 K, while the temperature of the second (or cold) stage is 10–20 K. The first stage is connected to the 80 K cooling area, while the second stage is connected to a 15 K cooling area.

Cryopumps, as entrapment pumps, do not show a gas throughput, but rather accumulate gases by freezing them out at their cold surfaces. For that reason, there are two peculiarities in the operation of cryopumps. The first one is the use of roughing pumps. They are required, but operate only during pump-down to fore-vacuum pressures. During the high vacuum pumping phase of a cryopump, the roughing pump is shut down. The second is the need for regular regeneration, to defrost the cryopump's cold surfaces.

Due to the necessity of a regular regeneration, a cryopump does not support pumping corrosive gases. Uncontrolled levels of such corrosives would occur during regeneration.

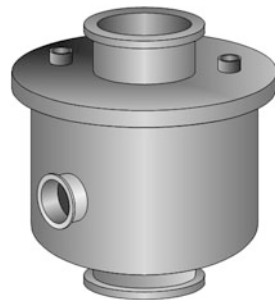
As mentioned before, cryopumps create a highly contamination-free vacuum. They achieve a pumping speed as high as  $10^7$  l/s, which is the highest for all high vacuum pumps [1] and reach pressures of  $0.1\text{--}10^{-8}$  Pa ( $7.5 \times 10^{-4}\text{--}7.5 \times 10^{-11}$  Torr) [13].

### 2.7.2 Cryogenic Pumps II—Meissner Trap

As discussed above, the bulk of the gas load to be pumped is water. An inexpensive cryo solution to increase the pumping speed is to add a liquid nitrogen ( $\text{LN}_2$ ) cooled cold trap. Although a cryogenic technology, the use of  $\text{LN}_2$  with a temperature of 77 K is much less complex and costly than the use of liquid He with a temperature of 4 K as used for cryopumps. Furthermore,  $\text{LN}_2$  is available worldwide, practically, in every thin-film fab. A Meissner trap with an area of a given size inside a vacuum chamber acts like a perfect pump for water vapor with an aperture of the same size [30]. If positioned unobstructed inside the vacuum chamber, the effectiveness of the Meissner trap is 100 %. The disadvantage of the Meissner trap is the need to warm it up and defrost it each time when the vacuum is broken.

Figure 2.24 schematically shows a hollow, double-walled Meissner trap. The space between two walls is filled with  $\text{LN}_2$ , which leads to the condensation of water and other gases at the inner wall.

**Fig. 2.24** Meissner trap  
(adapted from Pink GmbH  
Vakuumtechnik)



### 2.7.3 Getter and Sputter Ion Pumps

Getter pumps and sputter ion pumps are capture pumps [1]. They create pumping action by capturing gas molecules. They may getter (react with) chemically active gases or bury them below the surface. Getter and sputter ion pumps are applied as auxiliary pumps, either to purge the vacuum of specific reactive gases detrimental for a certain process or to improve the general vacuum pressure as “clean” pumps. They are most useful in UHV applications where very clean conditions must be maintained over a long time. Examples are particle accelerators, electron microscopes, electron beam writers, and vacuum chambers for sensitive samples. This pump type is only able to operate at a pressure below approx.  $10^{-2}$  Pa ( $7.5 \times 10^{-5}$  Torr), therefore requiring a separate high vacuum system such as a rotary vane/turbomolecular pump combination for the pump process. Furthermore, it is not suited for a continuous gas flow.

#### 2.7.3.1 Titanium Sublimation Pump (TSP)

A titanium sublimation pump (TSP) is a getter pump. The reason Ti is chosen is because its sublimation temperature (i.e., its temperature, at which it changes from solid to vapor without passing through a liquid state) is much lower than for other metals and it reacts with a large number of gases.

Figure 2.25 schematically presents a Ti sublimation pump. An assembly of filaments of Ti is surrounded by a double-walled cylindrical reservoir cooled by water or liquid nitrogen. Heating the filaments electrically sublimates the Ti into the vacuum and deposits it on the cylinder wall. This fresh Ti layer has a high pumping speed for reactive gases and either forms a compound (e.g., TiO) or traps them. The pumping speed mainly depends on the sticking coefficient of the respective gas on the Ti surface. For example,  $H_2$  is pumped several times more effectively than  $O_2$ ,  $H_2O$ , or  $N_2$ , and several hundred times faster than Ar [13]. Unlike cryopumps, a titanium sublimation pump removes the gases permanently.

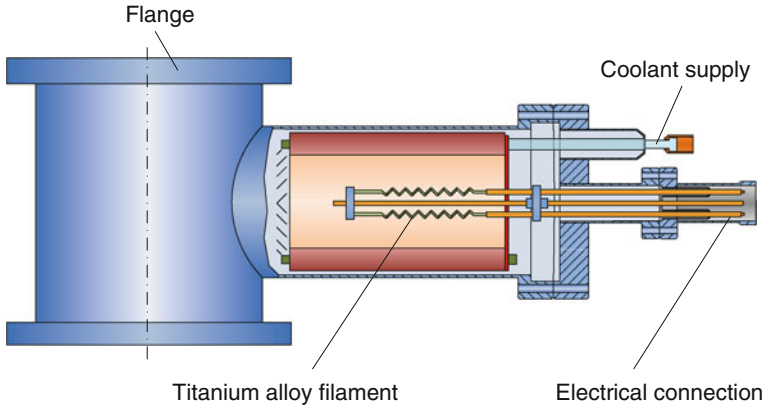


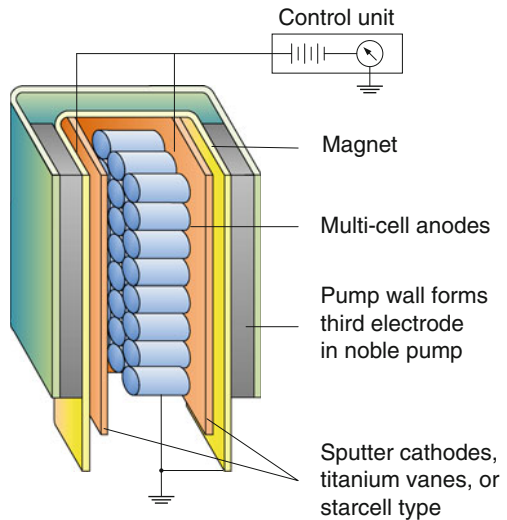
**Fig. 2.25** Titanium sublimation pump (adapted from Umrath [2])

### 2.7.3.2 Sputter Ion Pump

Figure 2.26 illustrates the schematics of a sputter ion pump. It achieves pumping by sorption processes initiated by ionized gas [13].

A cold cathode electrical discharge between an array of cylindrical stainless steel anodes and pairs of titanium cathode plates at each end emits electrons. This cold emission discharge process is similar to the one observed in a Penning gauge (see Sect. 2.9.4). The cathode potential against the anodes is in the range of a few kV. A transversal magnetic field with a flux density  $B$  of 0.1 T forces the electrons on spiral tracks, until they impinge on the anode. This results in a cloud of high

**Fig. 2.26** Sputter ion pump (adapted from Ohring [13])



electron density (e.g.,  $\sim 10^{10}$  electrons/cm<sup>3</sup>), causing collisions between the electrons and residual gas molecules. After the resulting impact ionization, the ions are accelerated towards the cathode and penetrate into the cathode, thereby sputtering atoms of Ti. These atoms deposit elsewhere in the pump, forming a highly reactive Ti film which getters reactive gases, such as N<sub>2</sub>, O<sub>2</sub>, and H<sub>2</sub>. Fresh layers of sputtered Ti bury these Ti compounds, as well as the ionized gas molecules embedded in the sputtering process. By paralleling many individual cold cathode arrangements, the sputter ion pump attains a sufficiently high pumping speed for the residual gases [2].

## 2.8 Vacuum Seals

Vacuum systems have to be designed and built in a way that there is no or very little gas leaking into them from the outside. Therefore, demountable joints and in particular flanged connections have to be air-tight. This is accomplished by using appropriate vacuum seals. A vacuum seal is undoubtedly one of the most important machine elements in vacuum systems. Figure 2.27 represents two commonly used seals, which will be discussed in more detail below.

### 2.8.1 Elastomer Seals

The most commonly used elastomer seals are O-rings. Their shape is mostly toroidal and their cross section circular. They allow leak-free flanges for pressure levels down

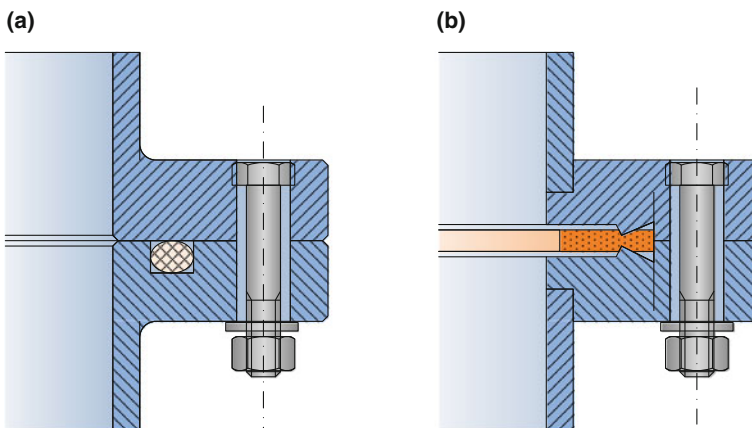


**Fig. 2.27** High vacuum seals (adapted from O'Hanlon [1]). **a** O-ring in rectangular groove. **b** ConFlat® type knife edge metal seal

to  $10^{-5}$  Pa ( $7.5 \times 10^{-8}$  Torr) [32]. They are placed either freely between two flat surfaces or confined in a groove with alternative cross sections (rectangular, triangular, or dove tail) [1]. An O-ring's suitability for high vacuum application strongly depends on its material's low vapor pressure at service temperature. To fulfill this requirement, it may not contain any components which may vaporize at service pressure. Specifically for large chambers (with diameters between 5 and 8 m), the preferred O-ring material is butyl, Buna-N, and fluorocarbon (Viton-A). The hardness of O-rings ranges from 65 to 80 Shore (measurement for hardness defined by Albert F. Shore). In the assembled state O-rings are compressed. A typical compression is 20 %. To ensure high vacuum sealing, typically a contact pressure of  $1.3 \times 10^6$  Pa is considered necessary [1]. Figure 2.27a shows a representative flange arrangement. Another way to decrease the leak rate is lubricating the O-rings with high vacuum grease. It improves sealing by filling up surface imperfections like pits and grooves at the mating surfaces.

Another important feature is a high material resistance to gas permeation [1]. Compression not only improves sealing, it also reduces permeability. This is due to the fact that compression both reduces the area available for the entry of gas as well as increases the length of the path the gas has to travel.

The cross section diameter (thickness) of the O-rings ranges from 2 to 12 mm. A preferred diameter used for many joints is 5 mm; rings with thicknesses of 8–12 mm are used only for very large seals.

### 2.8.2 Metal Seals

For applications in which the thermal, outgassing, and permeation properties of O-rings are unsatisfactory, metal gaskets lend themselves for being used. This is particularly true for ultrahigh vacuum (UHV) applications [1]. Materials frequently used for metal seals are copper, aluminum, indium, and, in some cases, silver or gold. A seal material used preferably in UHV systems is copper, typically used in conjunction with ConFlat<sup>®</sup> type knife edge flanges (Fig. 2.27b). For an elevated temperature application above 200 °C, silver-plated copper gaskets are used. The silver coating serves as a diffusion barrier against atmospheric oxygen, which would cause the copper to oxidize. Metal seals can be used only once.

## 2.9 Vacuum Measurement and Analysis

### 2.9.1 Introduction into Pressure Measurement

Pressure gauges are instruments for measuring the gas pressure [2]. Here we are only interested in gauges that operate below atmospheric pressure. We differentiate between those that measure the pressure  $p$  directly and those that measure it indirectly.

The pressure  $p$  is defined as the force  $F$  acting on an area  $A$ . As we have seen (see Sect. 2.1.3), this force only depends on the particle number density  $n$  and the temperature  $T$ , but not on their molar mass  $M$ . Therefore, if we measure the pressure directly, the measurement result is independent of the type of gas [2].

Instruments with indirect pressure measurement take advantage of some pressure contingent properties, e.g., the gas' thermal conductivity. These properties depend not only on the temperature  $T$ , but also on the molar mass  $M$ . Such a measurement is subject to the type of gas and has to be appropriately calibrated.

## 2.9.2 Direct-Reading Pressure Gauges

### 2.9.2.1 Bourdon Gauge

The most commonly used direct-measuring pressure gauge is a mechanical device, the Bourdon gauge, represented by Fig. 2.28 [1, 2]. It was invented by the French watchmaker and engineer Eugene Bourdon (1808–1884) in 1849 [33]. Figure 2.28a illustrates a Bourdon gauge's components. The sensing element is the Bourdon tube, a circular arc shaped tube of elliptical cross section, connected to a channel ending at the measurement site. Mechanically, the Bourdon tube is fixed at one end and connected to a pointer mechanism at the other. An evacuation causes a deflection of the Bourdon tube, resulting in the rotation of the pointer. Figure 2.28b shows a picture of a Bourdon gauge.

High-precision versions of the Bourdon gauge cover a pressure range from  $10^3$  to  $2 \times 10^5$  Pa (10–760 Torr). The sensitivity is in the order of 25 Pa (0.2 Torr) [1].

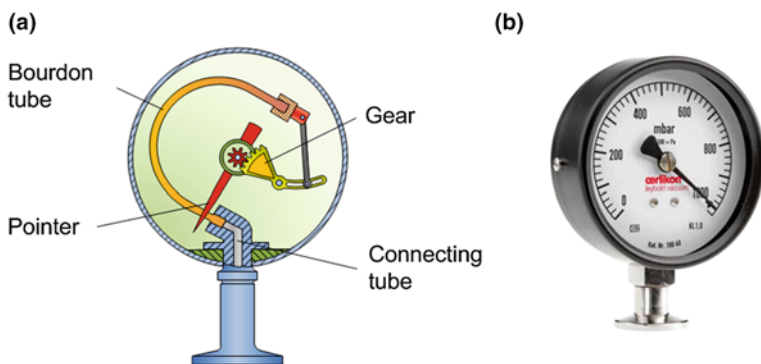


**Fig. 2.28** Bourdon gauge. **a** Schematic representation (adapted from Umrath [2]). **b** Photograph courtesy of Oerlikon Leybold Vacuum

### 2.9.2.2 Diaphragm Gauge

The diaphragm gauge contains a hermetically sealed, evacuated diaphragm capsule as the pressure sensitive element [1, 2]. A pressure reduction causes the diaphragm capsule to expand, deflecting the diaphragm. A gear converts the linear deflection in a rotation of the pointer. For accurate versions, pressure range and sensitivity are the same as for the Bourdon gauge.

### 2.9.2.3 Capacitance Manometer (“Baratron<sup>®</sup>”)

A capacitance manometer is a pressure gauge in which the deflection of a diaphragm is measured by the change in capacitance between it and a counter-electrode [1]. It is also known by its brand name Baratron<sup>®</sup>.<sup>4</sup> A capacitance manometer was originally suggested in 1951 by Alpert, Matland, and McCourby [34].

Figure 2.29 depicts a schematic representation of a Baratron<sup>®</sup> capacitance manometer’s sensor capsule [35]. It contains a radially tensioned metallic diaphragm and a metal-on-ceramic counter-electrode structure. Pressure is determined by measuring the capacitance between the metal diaphragm and the adjacent fixed dual-electrode. On one side of the diaphragm (the one whose pressure is to be measured), a baffle protects the delicate diaphragm. On the other side of the diaphragm is the reference side, which is also the capacitance measurement side. It is evacuated to a very high vacuum, much lower than the pressure to be measured. This way, a deviation of the gas’ dielectric constant to that of air does not influence the measurement result. One way to maintain high vacuum on this reference side over the manometer’s life is the integration of an internal chemical getter pump. The manometer is designed to be insensitive to overpressure; in case it

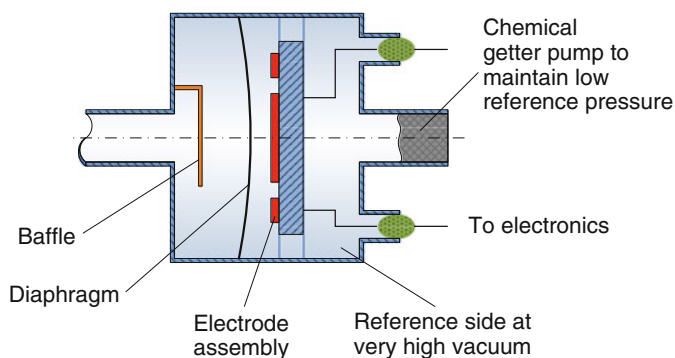


**Fig. 2.29** Capacitance manometer (“Baratron<sup>®</sup>”; adapted from MKS Instruments [35])

<sup>4</sup> Baratron<sup>®</sup> is a registered trademark of MKS Instruments, Andover, Massachusetts, USA.

occurs, the diaphragm will bottom out on the electrode substrate, preventing permanent damage to the sensor.

Capacitance manometers can be operated over a large dynamic range of typically  $10^4$  to  $10^5$  [1]. A typical measurement range for a transducers with a full-scale deflection of 130 Pa (1 Torr) is  $2.5 \times 10^{-2}$  to  $6.5 \times 10^{-4}$  Pa ( $1.9 \times 10^{-4}$ – $5 \times 10^{-6}$  Torr).

### ***2.9.3 Indirect-Reading Gauges—Thermal Conductivity Gauges***

Since the pressure in a vacuum chamber passes through up to 13 orders of magnitude during pump-down, different measurement principles are necessary to cover the pressure regimes all the way from the viscous flow regime towards the molecular flow regime. For the viscous flow regime at a pressure above 0.1 Pa ( $7.5 \times 10^{-4}$  Torr), gauges measuring the momentum transfer by gas molecules are well suited. Thermal conductivity gauges measure the rate of heat transfer between a hot wire and its surroundings [1]. Since the heat transfer also depends on the molecular mass of the gas, a specific calibration is required.

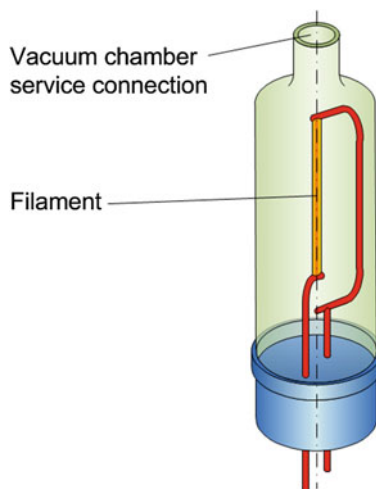
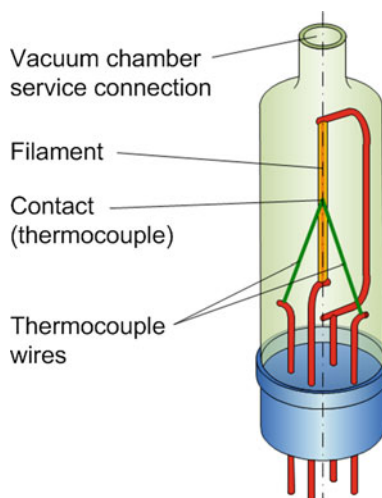
#### **2.9.3.1 Pirani Gauge**

Any pressure gauge with a heated wire, which forms one arm of a Wheatstone bridge is called Pirani gauge [1]. The Pirani gauge was invented in 1906 by Marcello Pirani (1880–1968), a German physicist [36]. Figure 2.30 shows a Pirani gauge. The heating elements and its leads are protected by a vacuum tube which is open at its top to allow access to the vacuum. The wire, which is subject to Joule's heating (heating a conductor by the flow of an electric current) at constant power reaches a steady-state temperature. This temperature is a function of thermal conductivity of the gas. A decrease in pressure results in a reduction of heat flow and thus a temperature rise at the heater. By measuring the heated wire's resistance  $R$ , its temperature is determined and calibrated to the gas pressure. The Pirani gauge has a measurement range of  $10^4$ –0.1 Pa ( $75$ – $7.5 \times 10^{-4}$  Torr).

#### **2.9.3.2 Thermocouple Gauge**

Like the Pirani gauge, the thermocouple gauge measures temperature dependent heat flow [1]. While the Pirani gauge measures the heating element temperature directly by determining the element's temperature dependent ohmic resistance, the thermocouple gauge uses an extra element, a thermocouple, to measure the



**Fig. 2.30** Pirani gauge**Fig. 2.31** Thermocouple gauge

temperature of the filament. A thermocouple takes advantage of the Seebeck effect, discovered in 1821 by the Estonian-German physicist Thomas Johann Seebeck (1770–1831) [37]. It allows a direct conversion of a temperature difference to an electric voltage [1]. The thermoelement applied consists of two wires of different materials (e.g., Chromel and Alumel), spot welded to the heater element at mid-point. This represents the hot end of the thermocouple. Figure 2.31 schematically represents a thermocouple gauge. The thermocouple gauge has a measurement range of  $10^4$ – $0.1$  Pa ( $75$ – $7.5 \times 10^{-4}$  Torr).

### 2.9.4 Indirect-Reading Gauges—Ionization Gauges

In the high and ultrahigh vacuum region, the particle density is too low to allow a reliable pressure measurement by momentum transfer [1]. Therefore, in a region below  $10^{-3}$  Pa ( $7.5 \times 10^{-6}$  Torr), pressure is measured by ionizing gases and measuring the discharge current.

#### 2.9.4.1 Penning Gauge

The Penning gauge (Fig. 2.32) is a cold cathode gauge invented in 1937 by the Dutch physicist Frans Michel Penning (1884–1953) [38, 39]. Inside a glass tube which is open at its top, a pair of cold cathodes emits electrons which travel towards a hollow cylindrical anode [1]. The voltage between cathode and anode is 2–10 kV. A pair of permanent magnets outside the glass tube creates a magnetic field. The arrangement of electric and magnetic fields forces the electrons into a spiral path. This way, they travel long distances with a sufficiently high likelihood of collisions with gas molecules even at low pressures, before they impact on the anode. To cause a discharge, an electron or ion has to have gained enough energy to ionize a gas molecule. The resulting positive (ions) and negative (electrons) charge carriers travel to the respective electrodes and provide a discharge current. The pressure can be derived from the current. Yet, the gauge needs to be calibrated as the current is temperature dependent and also depends on the gas species. The range of operation of a Penning gauge is  $1\text{--}10^{-9}$  Pa ( $7.5 \times 10^{-3}$  to  $7.5 \times 10^{-12}$  Torr).

**Fig. 2.32** Penning type cold cathode discharge tube

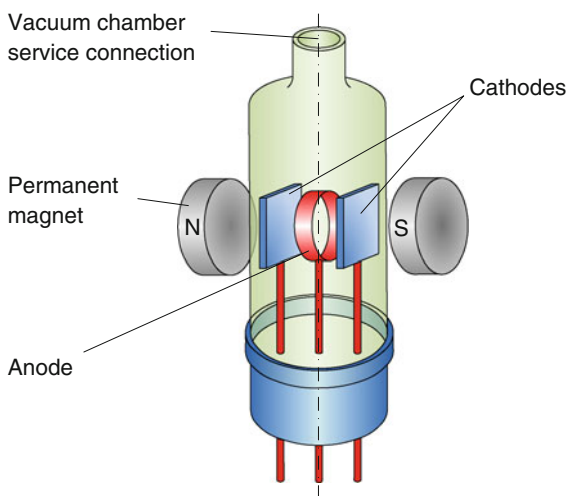
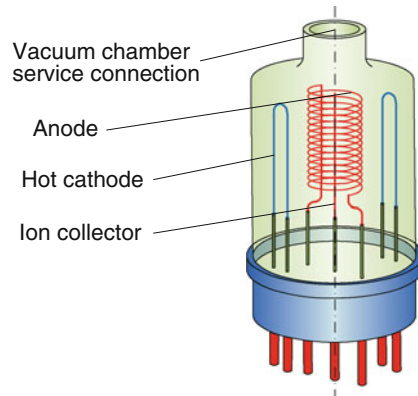


**Fig. 2.33** Bayard-Alpert ionization gauge tube



### 2.9.4.2 Bayard-Alpert Gauge

The Bayard-Alpert gauge is a hot filament pressure gauge designed in 1950 by Robert T. Bayard and Daniel A. Alpert (Westinghouse Research Laboratories, Pittsburgh, Pennsylvania, USA) [40]. A hot filament is an abundant electron source. Figure 2.33 illustrates a Bayard-Alpert pressure gauge. The system shown has a pair of hot filaments located outside a spiral shaped anode. At the anode's center is a thin wire serving as ion collector. Electrons emitted from the hot filaments are accelerated in an electric field created by the anode and gain enough energy to ionize gas molecules. The positive gas ions travel to the negatively charged ion collector to which they transfer their charge upon impact. Compared to a Penning gauge, the surface of the ion collector is rather small. Therefore, the creation of photoelectrons due to X-ray effects is greatly reduced. For a modulated Bayard-Alpert gauge, the X-ray limiting pressure is  $9 \times 10^{-9}$  Pa ( $7 \times 10^{-12}$  Torr).

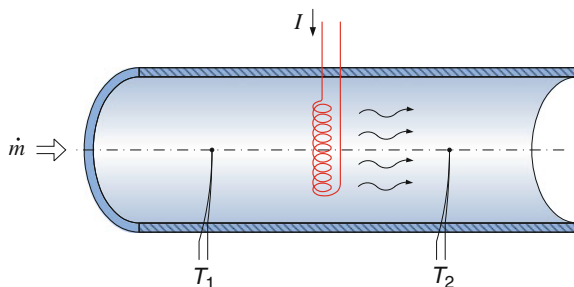
## 2.9.5 Flow Meter and Mass Flow Controller

### 2.9.5.1 Mass Flow Meter

For quite a few vacuum processes, the reduced pressure atmosphere consists of a process gas. This may be argon as a plasma gas for sputtering or a combination of argon and precursor gases in case of a PECVD. The respective process gas enters the vacuum chamber through a special port at predetermined rates, measured by a mass flow meter.

The most commonly applied principle is the thermal mass flow measurement, invented in 1911 by Thomas (Fig. 2.34) [1, 41]. An electric heating element, excited at constant power by Joule's heating, transfers thermal energy to the gas. It heats the gas. An upstream thermometer measures the gas temperature before heating, while a

**Fig. 2.34** Thermal mass flow meter schematics (adapted from O'Hanlon [1])



downstream thermometer allows measuring the temperature rise. The heat transfer is linearly dependent on the mass flow and the gas' specific heat [1].

### 2.9.5.2 Mass Flow Controller

A mass flow controller is a device that keeps the mass flow at a desired level. A mass flow meter as described above provides its measurement input. Additionally, it features a valve which influences the mass flow and an electronic control circuitry opening the valve to the desired level.

## 2.9.6 Residual Gas Analysis (RGA)

### 2.9.6.1 Introduction

Residual gas analysis (RGA) is a proven technique for the solution of many vacuum related fabrication issues [1]. It is a sophisticated process control instrument used extensively for diagnosis purposes and for verifying environments. Applications are the measurement of gas purity, gas contaminations initiating from films and sputtering targets, and vapor fluxes from physical vapor deposition sources, to name just a few. The measurement principles applied in RGA is mass spectrometry.

### 2.9.6.2 Mass Spectrometry Basics

Figure 2.35 schematically shows a mass spectrometer used in the RGA and its three stages: ionizer, mass separator, and detector, all operating under vacuum conditions. The first step of gas analysis is to ionize the gas taken from the vacuum chamber. This is a basic necessity, because only ionized gas atoms are electrically charged and thus able to be accelerated or deflected by electric or magnetic fields. Shown in our case is a hot filament ionizer, a profuse electron source with excellent ionization capabilities. After their ionization, the gas ions are accelerated by an electric field

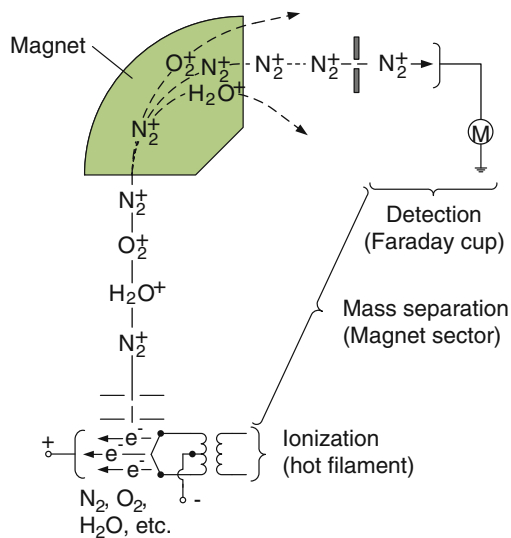


**Fig. 2.35** Mass spectrometer for residual gas analysis (adapted from O'Hanlon [1])

towards the mass filter. The one shown is a magnetic sector mass filter. The system contains a 90° circular channel surrounded by an electromagnet. Depending on the chosen magnetic field strength  $H$  applied in vertical direction and the gas molecules' mass, the molecules travel on circular paths of various radii, with heavier molecules on a larger radius and lighter ones on a smaller one. For a given magnetic field  $H$ , only one species will travel on a particular radius. In our example,  $N_2^+$  passes the channel right at the center. It then travel through a slot at the entrance of a detector. The detector shown is a Faraday cup—a conductive can catching charged particles in vacuum and converting them into a current. By varying the magnetic field strength  $H$  of the electromagnet, all species are admitted sequentially to the Faraday cup, thus providing information regarding the residual gas composition.

A mass filter quite commonly used in RGA is the RF quadrupole [1, 13], invented by the German physicist Wolfgang Paul<sup>5</sup> and coworkers [42]. Figure 2.36 illustrates its ideal geometry (Fig. 2.36a) as well as the path of the filtered ions (Fig. 2.36b). Ideally, the electrodes are hyperbolic in cross section. However, for technical applications, they are facilitated by four rods with cylindrical cross sections. Opposite electrodes are at the same potential, consisting of a plus or minus DC potential with a superposed high-frequency AC potential.

Due to a potential valley created by the two rods with positive DC potential near the axis of symmetry, positive ions are possibly stable. However, ions with a low mass to charge ratio  $m/z$  are able to follow the periodic component of the field. The

<sup>5</sup> Shared Nobel Prize in Physics 1989.

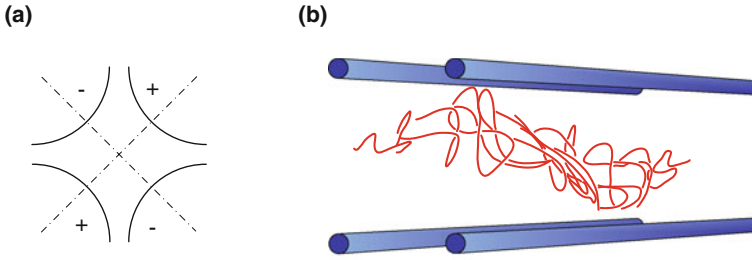
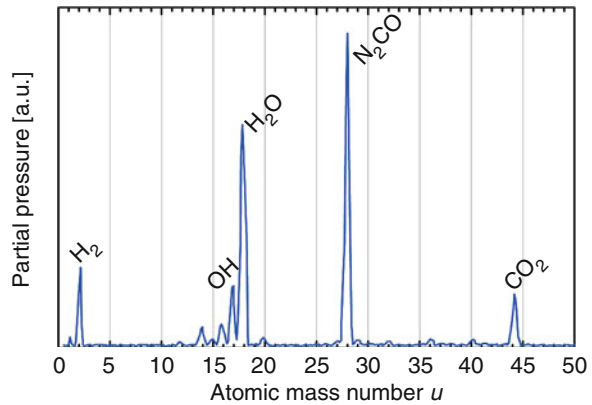


**Fig. 2.36** Quadrupole mass filter. **a** Idealized hyperbolic electrode cross section. **b** Schematic electrode arrangement and example of a stable ion path. *Source* O'Hanlon [1], used with permission

**Fig. 2.37** Quadrupole ultrahigh vacuum analysis result. *Source* MBE, Leibniz Universität Hannover



lower the mass to charge ratio, the greater is the ions' capability of gaining energy from the periodic field. As a result, their amplitudes increase, until they impact at the rods and discharge. Since only ions with a high charge to mass ratio are able to pass, this part of the quadrupole is a *high-pass mass filter*. The pair of rods with a negative potential cause a deflection of the ions with a high charge to mass ratio, also resulting in an impact at the rods. This part of the system represents a *low-pass mass filter*: only ions with a large charge to mass ratio  $M/z$  are able to pass. Jointly the two filters form a band-pass mass filter. By choosing an appropriate combination of DC and AC voltages, only ions with a characteristic mass to charge ration  $m/z$  will pass through the quadrupole's center, all others are filtered out. Figure 2.37 presents a quadrupole mass spectrum of a molecular beam epitaxy (MBE) system's ultrahigh vacuum.

## 2.10 Desorption and Leaks

### 2.10.1 Gas Release from Solids

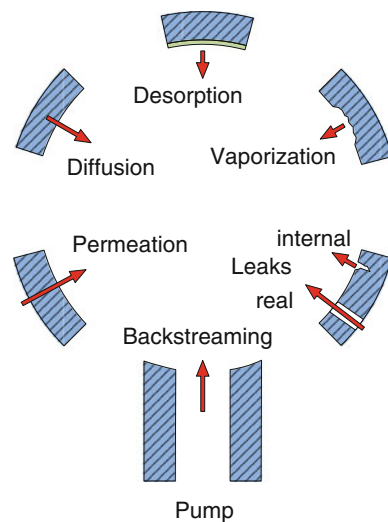
The vacuum system obviously has to remove gas particles from inside the vacuum chamber. However, this is by far not all that has to be pumped. Besides the volume gas, there are various sources of surface gas that have to be removed [1]. Typically, surface gas is released slowly in a process called outgassing. Several processes contribute to outgassing, as demonstrated by Fig. 2.38. They are vaporization, diffusion, thermal desorption, stimulated desorption, and permeation. Additionally, there may be gas penetration through leaks as well as gas backstreaming from the pump system. Due to all of these effects there is a minimal pressure a vacuum system can reach. This minimal pressure is dictated by the equilibrium between pump rate and outgassing rate.

#### 2.10.1.1 Vaporization

Vaporization is the process of a substance reaching a state above its condensation temperature by thermal stimulation [1]. Therefore, prior to a pump-down process, liquid films and solids are vaporized intentionally. The evaporation of solids under vacuum conditions is a function of the material's temperature, vapor pressure, surface area, and molecular weight [1].

As mentioned previously, it is water that constitutes for the bulk of the gas load in the high and ultrahigh vacuum regimes. However, removing this water typically is not accomplished in an evaporation process, but rather by desorption, (see below) [43].

**Fig. 2.38** Outgassing sources  
(adapted from O'Hanlon [1])



### 2.10.1.2 Diffusion

Diffusion is a transport phenomenon where one material passes through another driven by a material concentration gradient. For vacuum chambers, it is caused by a significant pressure difference between outside (atmospheric pressure) and inside (vacuum) [1]. The gas diffuses towards the inside and desorbs from the wall surface into the chamber. Of these two processes involved, desorption typically is much faster than diffusion. Therefore, it is typically the diffusion rate through the bulk which determines the rate of outgassing into the vacuum.

### 2.10.1.3 Thermal Desorption

Thermal desorption is the heat-induced discharge of gases and vapors that were previously adsorbed at the vacuum chamber's wall surfaces [1]. There are alternative causes for a previous absorption having taken place: (i) adsorption may have occurred during a previous breaking of the vacuum, during which the vacuum chamber was exposed to atmospheric pressure. (ii) Molecules may have reached the inner recipient surface by diffusion from within, as described above. (iii) The source of adsorbed material is permeation, which still has to be discussed (see below). In any case, the bonding of gas molecules to the surface occurred either by physisorption or chemisorption. The desorption rate depends on the molecular binding energy, as well as surface temperature and surface coverage.

This is particularly true for water molecules. For water to be pumped away requires to being first released from the surface [43]. Binding energies of water lie between those of weak van der Waals bonds and true chemical bonds. Breaking these bonds may be instigated by thermal desorption, caused by thermal heat transfer from the chamber walls.

### 2.10.1.4 Stimulated Desorption

Stimulated desorption is the release of gas or vapor caused by electron, atom, molecule, or photon incidents and may be large enough to limit the ultimate pressure of a vacuum chamber [1]. Among them are electron-stimulated desorption, ion-stimulated desorption, electron-stimulated or ion-stimulated chemical reaction, and photodesorption. Electron-stimulated desorption, for instance, is caused by an energetic electron incident which excites a bonding electron in an adsorbed atom to a non-bonding level. An example of ion-stimulated desorption is the release of a chemically bonded gas molecule by an incident of a noble gas atom. Stimulated chemical reactions typically occur on solid surfaces, e.g.,  $H_2$  and  $O_2$  reacting with solid C to produce  $CH_4$  (methane) or CO. An example for photodesorption is desorption due to optically induced surface heating.



### 2.10.1.5 Permeation

Permeation is the passage of gases through metallic or non-metallic solids. The process sequence resulting in permeation is adsorption at the chamber wall at the high pressure side, diffusion through the bulk wall material, and desorption from the wall at the low pressure side. This process is highly temperature dependent. Permeation may be molecular or atomic. For glass, ceramic, and polymeric materials, molecules do not dissociate during permeation. On the other hand,  $H_2$  dissociates on metal surfaces, diffuses as atoms, and recombines before desorption inside the vacuum chamber at the vacuum wall.

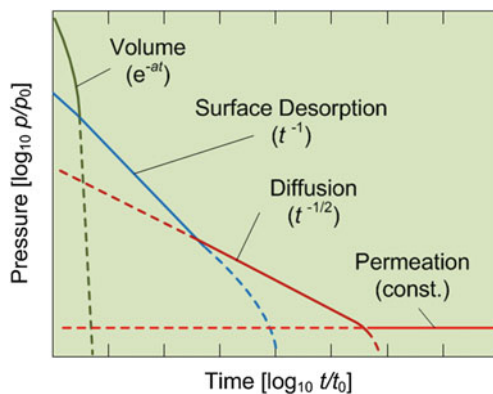
### 2.10.1.6 Gas Release During High Vacuum Pumping

Figure 2.39 shows high vacuum pumping under the influence of outgassing. The system shown is unbaked and has metal gaskets [1]. The initial phase represents volume gas removal, the pressure reduces exponentially. This phase takes only seconds, but is shown extended for clarity.

Surface desorption governs the rate of pressure decrease in the next phase, in which the pressure typically decreases proportional to  $t^{-1}$ . Being an unbaked system, most of the gas load is water vapor. The inner part of a glass or steel vacuum chamber that has been exposed to atmospheric pressure may contain up to 100 monolayers of water vapor (this is the reason for the preferred use of loadlocks, see Sect. 2.4.1). Furthermore, a slow decrease of pressure may be expected if the system has a number of large O-rings or a large interior surface area.

In the diffusion governed range, the pressure decrease is initially proportional to  $t^{-1/2}$ . Permeation dictates the ultimate achievable pressure, with equilibrium between the ultimate high vacuum pump gas removal rate and the permeation rate. Obviously, this stage is only reached if the system is free of leaks.

**Fig. 2.39** Rate limiting effects during the pumping of a vacuum chamber. *Source* O'Hanlon [1], used with permission



## 2.10.2 Leaks and Leak Detection

### 2.10.2.1 Type of Leaks

As already discussed previously, vacuum systems are very sensitive to gas leakage. While no vacuum system can ever be absolutely vacuum-tight (and actually does not need to be) [2], any major leak jeopardizes a proper system function.

Let us first look at sources for leaks [2]. One way to differentiate between them is to look at the nature of the material or joint at fault.

(i) *Leaks in detachable connections* include flanges, ground mating surfaces, and covers, while (ii) *leaks in permanent connections* comprise solder and welding seams as well as joints with adhesive bonding. (iii) *Leaks due to porosity* particularly may occur following mechanical deformation (bending) or thermal processing of polycrystalline materials and cast components. (iv) *Cold-warm transition leaks* may open up at extreme temperatures, particularly at solder joints. (v) *Internal (virtual) leaks* occur in case quantities of gas will be set free from cavities inside cast parts, blind holes, and creases. This may also occur due to the evaporation of liquids [2]. (vi) *Indirect leaks* may be caused by leaking supply lines in vacuum systems or furnaces. (vii) *Serial leaks* occur at the end of several spaces located one behind the other, for instance a leak in the oil-filled section of the oil pan in a rotary vane pump. (viii) *One-way leaks* will allow gas to leak in one direction but are tight in the other direction. This type of leak occurs rarely.

### 2.10.2.2 Leak Detection

Big leaks in vacuum systems can be detected by rather primitive methods, for instance by pressurizing the vacuum chamber with nitrogen and applying a water-soap mixture from the outside to suspicious areas and components. At the leak site, bubbles will occur. The most sensitive method for leak detection in high and ultrahigh vacuum systems is applying a tracer (sniffer) gas, preferably helium, at the suspected leak site and detecting it after passing the leak by using mass spectrometry [2]. The helium molecule is much smaller than a water or air molecule, so small that it can penetrate easily through a small leak. Furthermore, helium is chemically inert, non-explosive, non-toxic, and is present in normal air in a concentration of only 5 ppm. Vacuum testing is best performed “outside-in” [44]. To do so, the vacuum chamber is evacuated by its vacuum pump system. Helium is administered to the suspected leak sites using a spray probe with an adjustable flow. A helium spectral readout at the mass spectrometer provides the leak rate at the test site, indicating that the leak (or at least one of them) has been found.

## 2.11 Vacuum Pump Applications

### 2.11.1 Selection

Figure 2.40 represents a typical vacuum system for high vacuum or ultrahigh vacuum applications [2]. It consists of a vacuum chamber, a high vacuum pump, a roughing pump, and their respective connecting ducts and valves. In the selection of a vacuum pump system, the first question is what vacuum range has to be reached. Figure 2.41 provides an overview over the pressure ranges of all pumps discussed. Required pump throughputs shall not be discussed here. Vendors will offer advice.

A common choice for a roughing pump used in micro and nano fabrication applications with no concern for hydrocarbon backstreaming is the rotary vane pump. In case it is applied in vacuum tools operating with corrosive gases, the pump will be lubricated with Fomblin<sup>®</sup> right after its fabrication. For high vacuum pumps, the options typically are between a cryopump, turbomolecular pump, or turbomolecular drag pump. For processes with non-corrosive gases, any of those pumps may be applied. The cryopump excels in robustness. However, it requires regular regeneration and is not to be utilized for pumping in corrosive processes. Turbomolecular pumps with and without drag stage may be used for corrosive processes, as long as the bearings are protected from corrosive gases. A turbomolecular drag pump is most prominently used in conjunction with a diaphragm pump and its limited fore-vacuum pressure in hydrocarbon-free systems. Getter and ion pumps may be applied to selectively lower the partial pressure of certain species (like reducing the residual O<sub>2</sub> content by applying a titanium sublimation pump). They are also used for achieving an optimal pressure in critical areas of a vacuum system (like further improving the pressure in the field emission cathode area of an electron microscope).

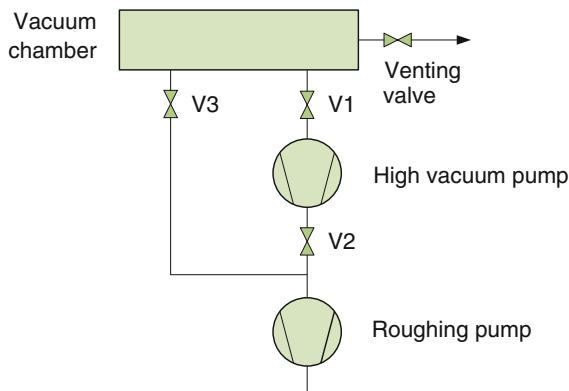


**Fig. 2.40** Typical vacuum system for high vacuum or ultrahigh vacuum applications. V1 through V3 are valves (adapted from Umrath [2])

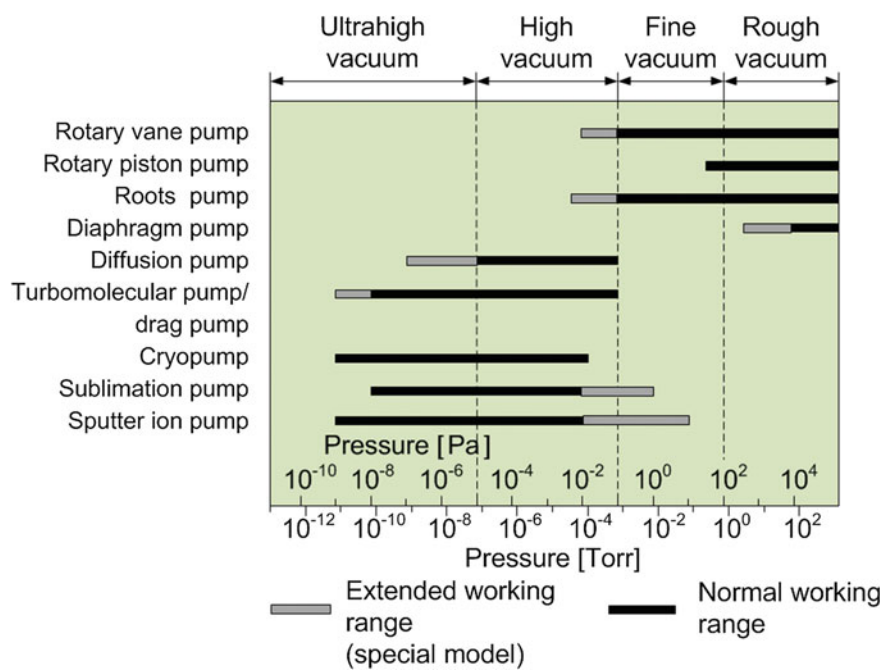


Fig. 2.41 Vacuum pump operating ranges (adapted from Umrath [2])

2.11.2 Examples of Vacuum Systems Used in Research

Table 2.3 presents four typical systems that require pumping, the vacuum pumps they are equipped with, and the pressure gauges they use. They are in use at the IMPT at the Leibniz Universität Hannover’s Center for Production Technology in Garbsen, Germany. The first vacuum system is a regular sputtering tool equipped with a loadlock. Its roughing pump is a rotary vane pump, its high vacuum pump is a cryopump. Operating a titanium sublimation pump specifically allows reducing the content of O<sub>2</sub> and other gases in the vacuum chamber. The second vacuum system is also a sputtering tool, this time capable of reactive sputtering, and also equipped with a loadlock. It combines a Fomblin<sup>®</sup> lubricated rotary vane roughing pump with a turbomolecular drag pump. The system has been used occasionally for reactive sputtering, among other for creating FeTaN films. In this process, the N<sub>2</sub> was administered jointly with the sputter gas Ar. The third system is an evaporation tool. It combines a rotary vane roughing pump with a turbomolecular pump. Finally we discuss the pump system of a PECVD. Due to its rather high operating pressure, it uses a combination of a Fomblin<sup>®</sup> lubricated rotary vane roughing pump with a roots pump, but no high vacuum pump.

**Table 2.3** Examples of vacuum systems applications

System	Sputtering (non-reactive)	Sputtering (reactive)	Evaporation	PECVD
Volume recipient	80 l	80 l	135 l	5 l
Process pressure	$10^1$ – $10^{-1}$ Pa ( $7.5 \times 10^{-2}$ – $7.5 \times 10^{-4}$ Torr)	$10^1$ – $10^{-1}$ Pa ( $7.5 \times 10^{-2}$ – $7.5 \times 10^{-4}$ Torr)	$10^{-4}$ Pa ( $7.5 \times 10^{-7}$ Torr)	66.7–133 Pa (0.5–1 Torr)
Loadlock	Joint		No	No
Roughing pump	Rotary vane	Rotary vane (Fomblin <sup>®</sup> )	Rotary vane	Rotary vane (Fomblin <sup>®</sup> )
Type	Balzars DUO 030A	Balzars DUO 030A	Leybold 065B	Alcatel 2033C2
Nominal pump rate	38 m <sup>3</sup> /h	38 m <sup>3</sup> /h	65 m <sup>3</sup> /h	30 m <sup>3</sup> /h
Final pressure	$1 \times 10^{-2}$ Pa ( $7.5 \times 10^{-5}$ Torr)	$1 \times 10^{-2}$ Pa ( $7.5 \times 10^{-5}$ Torr)	$2 \times 10^{-1}$ Pa ( $1.5 \times 10^{-3}$ Torr)	$2 \times 10^{-1}$ Pa ( $1.5 \times 10^{-3}$ Torr)
Booster pump	N.A.	N.A.	N.A.	Roots
Type	–	–	–	Alcatel R301 B
Nominal pump rate	–	–	–	300 m <sup>3</sup> /h
Final pressure	–	–	–	$2 \times 10^{-1}$ Pa ( $1.5 \times 10^{-3}$ Torr)
Fore-vacuum pressure gauge(s)	Pirani	Pirani	Pirani	Pirani, Baratron <sup>®</sup>
High vacuum Pump	Cryo	Turbomolecular Drag	Turbomolecular	N.A.
Type	CTI	Pfeiffer TPH 1600	Pfeiffer T 1600	–
Nominal pump rate	On-Board 8 1,500 l/s (air)	1,500 l/s (N <sub>2</sub> )	1,300 l/s (N <sub>2</sub> )	–

(continued)

Table 2.3 (continued)

System	Sputtering (non-reactive)	Sputtering (reactive)	Evaporation	PECVD
Final pressure	N.A.	$10^{-9}$ Pa ( $7.5 \times 10^{-12}$ Torr)	$3 \times 10^{-8}$ Pa ( $2.3 \times 10^{-10}$ Torr)	–
Getter pump	Ti Sublimation	N.A.	N.A.	N.A.
Type	AML Model TSP2	–	–	–
Gases to be pumped	O <sub>2</sub> , N <sub>2</sub> , CO <sub>2</sub>	–	–	–
High vacuum pressure gauge	Bayard-Alpert	Bayard-Alpert	Penning	N.A.
System pumpdown to final pressure (typical)	5–10 min (rough) + 5 min (high)	5–10 min (rough) + 30 min (high)	5–10 min (rough) + 30 min (high)	5 min (typical)

Source IMPT, Leibniz Universität Hannover

## Exercises

### 1. Vacuum

- a. What, strictly speaking, is vacuum?
- b. Can it be reached on earth?
- c. What do we really mean when we talk about vacuum?
- d. What are vacuum pressure regimes?

### 2. Vacuum pumps

#### 2.1 General

- a. There are two ways of classifying vacuum pumps—by pressure range and by pump principle. Name the respective groups and explain their features.

#### 2.2 Sketch the following vacuum pumps, label their key components, explain their work principle, specify their pressure range, and name advantages as well as (if present) disadvantages:

- b. Rotary vane pump
- c. Roots pump
- d. Membrane pump
- e. Diffusion pump
- f. Cryo pump
- g. Turbomolecular pump
- h. Turbomolecular drag pump
- i. What is the difference in work principle between a Holweck and a Siegbahn drag pump?

#### 2.3 What is a typical application of a

- j. Titanium sublimation pump
- k. Ion sputter pump
- l. Meissner trap.

### 3. What is the most commonly used seal?

### 4. Pressure gauges

#### 4.1 Sketch the following pressure gauges, label their key components and explain their work principle:

- a. Baratron<sup>®</sup>
- b. Bayard-Alpert
- c. Bourdon
- d. Penning
- e. Pirani
- f. Thermocouple

4.2 Which ones of the gauges are intended for operation in the following flow regimes:

- g. Viscous flow
- h. Molecular flow.

5. Outgassing

List outgassing sources.

6. Vacuum system

Sketch schematically and label a typical vacuum system.

## References

1. O'Hanlon JF (2003) A user's guide to vacuum technology, 3rd edn. Wiley, New York
2. Umrath W (2009) Fundamentals of vacuum technology. Oerlicon Leybold Vacuum, Cologne
3. Lederman L (2006) The god particle: if the universe is the answer, what is the question?. Houghton Mifflin, New York
4. Editors Encycl Britannica (2013) Evangelista Torricelli. <http://www.britannica.com/EBchecked/topic/600149/Evangelista-Torricelli>. Accessed 12 April 2014
5. Van Heiden A (2013) Galileo. Encycl Britannica. <http://www.britannica.com/EBchecked/topic/224058/Galileo>. Accessed 12 April 2014
6. Redhead PA (1999) History of vacuum devices. CAS—CERN Accelerator School: Vacuum Technology, Snekersten, Denmark, pp 281–290
7. Editors Encycl Britannica (2013) Otto von Guericke. Encycl Britannica. <http://www.britannica.com/EBchecked/topic/248259/Otto-von-Guericke>. Accessed 12 April 2014
8. Schott G (1657) Mechanica Hydraulico-Pneumatica. Wikimedia Commons. <http://en.wikipedia.org/wiki/File:Magdeburg.jpg>. Accessed 23 March 2012
9. Wolf F (1964) Gaede, Wolfgang. Deutsche Biographie (German Biography). <http://www.deutsche-biographie.de/sfz19730.html>. Accessed 14 April 2014
10. Volta effect (2012) Merriam-Webster. <http://www.techniklexikon.net/d/volta-effekt/volta-effekt.htm>. Accessed 24 April 2012
11. Henning H (2007) Gaedes rotierende Quecksilberpumpe (The rotating mercury pump of Gaede). Vak Forsch Prax 9:27–31
12. Grigul U (1973) Technische Thermodynamik (Technical thermodynamics), 2nd edn. de Gruyter, Berlin
13. Ohring M (2002) Material science of thin films, deposition and structure, 2nd edn. Academic Press, San Diego
14. Price LM (2013) Robert Boyl. Encycl Britannica. <http://www.britannica.com/EBchecked/topic/76496/Robert-Boyle>. Accessed 14 April 2014
15. Editors Encycl Britannica (2013) Edme Mariotte. Encycl Britannica. <http://www.britannica.com/EBchecked/topic/365450/Edme-Mariotte>. Accessed 14 April 2014
16. Crosland MP (2013) Joseph-Louis Gay-Lussac. Encycl Britannica. <http://www.britannica.com/EBchecked/topic/227390/Joseph-Louis-Gay-Lussac>. Accessed 14 April 2014
17. Coley NG (2014) Amelio Avogadro. Encycl Britannica. <http://www.britannica.com/EBchecked/topic/45884/Amedeo-Avogadro>. Accessed 14 April 2014
18. Editors Encycl Britannica (2013) Avogadro's number. Encycl Britannica. <http://www.britannica.com/EBchecked/topic/45889/Avogadros-number>. Accessed 14 April 2014
19. Editors Encycl Britannica (2013) Ludwig Eduard Boltzmann. Encycl Britannica. <http://www.britannica.com/EBchecked/topic/72401/Ludwig-Eduard-Boltzmann>. Accessed 14 April 2014



20. Editors Encycl Britannica (2014) Kinetic theory of gases. Encycl Britannica. <http://www.britannica.com/EBchecked/topic/318183/kinetic-theory-of-gases>. Accessed 15 April 2014
21. Ogródnik A (2007) Reale Gase (Real Gases), [http://dante.phys.chemie.tu-muenchen.de/de/vorlesung/pc1/SS2006/3\\_Ideale%20und%20Reale%20Gase.pdf](http://dante.phys.chemie.tu-muenchen.de/de/vorlesung/pc1/SS2006/3_Ideale%20und%20Reale%20Gase.pdf). Accessed 18 May 2012
22. Clark J (2010) Real Gases, <http://www.chemguide.co.uk/physical/kt/idealgases.html>. Accessed 18 May. 2012
23. Becker W (1958) Eine neue Molekularpumpe (A new molecular pump). *Vakuumtechnik* 7:149–153
24. Becker W (1966) Die Turbo-Molekularpumpe (Turbomolecular pump). *Vakuumtechnik* 15:211–218 and 254–260
25. Holweck F (2010) A Hero in Vacuum. Edwards vacuum particle newsletter. <http://www.edwardsvacuum.com/asia/newsletters/particles/0210/funfact.html>. Accessed 01 June 2012
26. Siegbahn M (2012) Biographical. Nobelprize.org. Nobel Media AB. [http://www.nobelprize.org/nobel\\_prizes/physics/laureates/1924/siegbahn-bio.html](http://www.nobelprize.org/nobel_prizes/physics/laureates/1924/siegbahn-bio.html). Accessed 29 May 2012
27. Siegbahn M (2010) A hero in vacuum. Edwards vacuum particle newsletter, April 2010. <http://www.edwardsvacuum.com/asia/newsletters/particles/0410/funfact.html>. Accessed 19 May 2012
28. Lesker KJ (2014) Turbomolecular and drag pumps: technical notes. Jefferson Hills, PA. <http://www.repairfaq.org/sam/vacuum/tmpnotes.htm>. Accessed 16 April 2013
29. Source: Pfeiffer Vacuum GmbH, Berliner Strasse 43, 35614 Asslar, Germany
30. Willey RR (2002) Practical design and production of thin films, 2nd edn. Marcel Dekker, New York
31. O'Hanlon JF (2003) A user's guide to vacuum technology, 3rd edn. 15 Cryogenic Pumps, 15.3 Refrigeration techniques. Wiley, New York, pp 272–273
32. NASA Preferred practices for design and test of robust systems (2010) Vacuum seals design criteria, NASA Practice No. PD-ED-1223, <http://engineer.jpl.nasa.gov/practices.html>. Accessed 29 May 2012
33. Bourdon E (2009) Florida Institute of Technology's history of science, Feb 2009, <http://historyofscience2009.blogspot.de/2009/02/eugene-bourdon.html>. Accessed 01 June 2012
34. Alpert T, Matland CG, McCoubry AO (1951) A null-reading absolute manometer. *Rev Sci Instrum* 22:370–371
35. Baratron<sup>®</sup> capacitance manometers (2012) MKS. <http://www.mksinst.com/docs/UR/barainfo2b.aspx>. Accessed 15 June 2012
36. Pirani MS (2009) A hero in vacuum. Edwards vacuum particle newsletter, <http://www.edwardsvacuum.com/asia/newsletters/particles/0909/funfact.html>. Accessed 1 June 2012
37. Editors Encycl Britannica (2014) Thomas-Johann Seebeck. Encycl Britannica. <http://www.britannica.com/EBchecked/topic/532353/Thomas-Johann-Seebeck>. Accessed 15 April 2014
38. Penning FM (1937) High vacuum gauges. *Physica* 4:71
39. de Groot W (1953) Obituary of FM Penning. <http://www.arjenboogaard.nl/penning.html>. Accessed 01 June 2012
40. Bayard RT, Alpert TC (1950) Extension of the low pressure range of the ionization gauge. *Rev Sci Instrum* 21:571–572
41. Thomas CC (1911) The measurement of gases. *J Franklin Inst* 172:411–460
42. Paul W (2013) Biographical. Nobelprize.org. Nobel Media AB. [http://www.nobelprize.org/nobel\\_prizes/physics/laureates/1924/siegbahn-bio.html](http://www.nobelprize.org/nobel_prizes/physics/laureates/1924/siegbahn-bio.html). Accessed 15 April 2014
43. Danielson P (2000) Sources of water vapor in vacuum systems <http://www.vacuumlab.com/Articles/Sources%20of%20Water%20Vapor.pdf>. Accessed 01 June 2012
44. Leak detection (2012) HSV Leak detection application note. <http://www.heliumleakdetection.net/>. Accessed 31 May 2012

Micro and Nano Fabrication

Tools and Processes

Gatzen, H.H.; Saile, V.; Leuthold, J.

2015, XXVI, 519 p. 357 illus., 54 illus. in color.,

Hardcover

ISBN: 978-3-662-44394-1